Prof Jonathan L. Bamber, Director
Bristol Glaciology Centre

School of Geographical Sciences
University Road
Bristol BS8 1SS
England
(0117 331 4129 (Direct)
Fax: 0117 928 7878
Email: j.bamber@bristol.ac.uk

05 February 2015

Dear Eric,

On the following pages you will find i) our response to the referees' comments and ii) a marked up version of the revised m/s that shows all the changes that have been made. These are extensive and substantive and include three new figures and two new tables to address the various comments from the referees. As a consequence, the paper has grown in length quite a bit. We apologise for the length of time it has taken to make these changes and to re-run a number of simulations, which, as explained before, was largely due to the departure of the lead author from academia and the move of one of the other key authors to a university in Australia. We believe that the revised m/s is a major improvement on the original submission.

Yours,

Jonathan

Reviewer One

We would like thank the reviewers for their helpful and insightful comments. Referee comments are in normal font in red and our reply in italics.

I was curious why it was decided to estimate a trend, instead of, for instance, monthly changes. A trend is a good model for some of the processes (i.e. GIA), but perhaps is a poor choice to represent processes such as surface mass balance since there can be significant inter-annual variability. Could you please comment on this?
This statement is correct but raises several issues that represent computational and data challenges. In our framework, we are simultaneously inverting seven years' worth of ICESat, ENVISAT, GRACE and GPS data at relatively fine spatial scale. To make this computationally feasible we must employ dimensional reduction and this is partly achieved with the use of stochastic partial differential equations and a Gaussian Markov random field approach. This is not sufficient alone and we need, therefore, to reduce the data sampling in space and or time. In effect we do both. As explained in the m/s we are working on a time evolving solution but this will be with annual resolution. Monthly or seasonal solutions are challenging because of i) the computational cost and ii) that some of the data does not adequately resolve sub-annual signals. The ICESat data, in particular, which provide the lowest error dh/dt estimate, must be estimated over 3 year means to produce adequate spatial coverage.

Why not explicitly use the posteriori correlations from the mascon solutions themselves? Additionally, in Luthcke's solution, a 2000 m elevation cutoff is dictated in the spatial correlation constraints. Is this explicitly considered in your analysis? I believe using the formal posteriori covariance matrix would be more favorable
The reviewer suggests using the full covariance matrix for GRACE. Unfortunately, these data were not available for the release we are using here. Regarding the elevation cutoff, we have been provided with a version where the 2000m cut-off was not applied. This was not explicitly mentioned in the paper and will be added to the revised version.

I believe a nice addition to the paper would be a Table which succinctly captures the processes and methodology. For instance, in this table it would be nice to list the following: 1. Observations (altimetry, GRACE, gps, etc) 2. State parameters (trend for GIA, ice dynamics, etc) 3. Weighting information on the observations (both diagonal and off-diagonal components) 4. Assumed apriori information on the state parameters (both diagonal and off-diagonal components). This would allow the reader to quickly assess exactly what is being done and what assumptions are being made.- Truly, there is some dependence on your solution with the choice of 3) and 4) in the above comment. Could you please remark on this, or provide some analysis on how sensitive the solution is to these choices? Additionally, there was no discussion of relative data weights. Do you weight any observations higher than others? What is the relative weight of the apriori information on the state relative to the observations? Some discussion of these matters would be appropriate.
This point was also raised by referee 2. Including a sensitivity analysis is possible and we will add a table as suggested in an updated version of the paper, and include a more detailed section regarding the sensitivity of the results to any data errors. However, we would like to stress at this point that there is no weighting applied to the observations.

The results that you presented left me wondering how well you are fitting the data. What are the RMS of the residuals? How does the misfit to each observation type look spatially? Is

your estimate fitting to one specific observation better than another? For instance, does your estimate agree better with altimetry than GRACE? If so, perhaps this was reflected in the initial choice of weights on the observations and choice of apriori information. This type of analysis would provide more credibility to the results presented.

How closely the results fit to a particular data set is, of course, a function of the a-priori error estimates that are associated with each dataset. As a consequence of this, we agree that it is important to discuss how these errors were estimated for each data set and we will expand the discussion of this in a revised m/s. It is not so easy to show a "misfit" between the data and the solution because the data are not observing one of the solved-for fields directly but some mixture of these fields. Altimetry does not observe a mass change but a volume change, for example.

What physical processes could allow for a negative SMB in this region?
Could you please comment more on this, and why this result is believable? "

We should have stressed that our results are trends on the SMB anomalies, so a negative signal represents a negative trend in the anomalies to a long-term mean. This could mean that, e.g. there is less snowfall over the 2003-2009 period than over the former years. As a consequence a –ve anomaly is just as plausible as a +ve one. We will clarify this in the text.

Reviewer Two

The reviewer is particularly concerned with the sensitivity of the approach to prior assumptions. Below we discuss this in some detail, and provide an outline of what will be included in the revised m/s.

Very little discussion on error analysis is provided. I think this should be addressed, particularly since the approach is statistically driven, so I would think error estimates for all of components would be available. The reader doesn't get a feeling for the errors for most of the input data sets and, other than the final ice mass loss values, none of the estimated components. Sigmas for the altimetry trends are given in Fig 2, but what are the uncertainties on the input GRACE mascons, the final SMB estimates, the final GIA rates? What is their spatial variation? Without this, it makes interpretation of the results and assessment of the comparisons more difficult (e.g., p3008 and p3009).

This point was also raised by the first reviewer and a subsection will be devoted to it in the revised m/s. This issue is exacerbated by the fact that we employ several data sets and provide solutions for several fields; a detailed analysis of all uncertainties will prove length and tedious to the reader. We will thus report the following:

a) We will plot a spatial map of the uncertainty associated with GRACE.

b) We will provide uncertainties over the summed contribution of SMB estimates, and the summed dm/dt due to GIA over the domain under study. These will be included in all of the comparisons (e.g. p3008 and p3009).

c) With regards to the spatial variation, we have stippled the mean plots where the field is deemed to be significant. This, together with what we report in b), we feel is sufficient. Plotting spatial uncertainties will increase the figure count by four and will considerably lengthen the manuscript.

Related to the first item, I would have liked to have seen more discussion on the influence of the various constraints that are employed (dh/dt error cutoff, static surface density, length scales, ice velocity constraint on elevation rates, etc.). I suspect that these have a significant influence on where the mass change is allocated within the framework, particularly the ice velocities constraint outlined on p.3004. What if a different constraint is used? What if no constraint it used?

The reviewer is correct in saying that our prior assumptions considerably affect the results. Several parameters are assumed known (e.g. surface density), and, moreover, we impose soft maxima for all processes which in turn are dependent on some prior belief on how these relate to the processes (for example the ice velocity constraint). On this point, putting no constraint will give a solution where the height change due to ice dynamics follows what is being observed in altimetry, since the spatial correlation length is relatively small. The ice velocity constraint helps to reduce this over-fitting and allocate height change in areas where ice velocity is low to other processes (in this case SMB and firn compaction). With regards to a difference constraint, the reviewer is right in saying that a different constraint will give different results. However, the aim of the framework is not to provide solutions which are independent of prior beliefs, rather to provide a solution under realistic prior assumptions (which could be verified using independent tests). Unfortunately, due to the under-determined nature of the system, estimating many of the parameters in our prior assumptions (for example the functional relationship of the constraint with respect to ice velocity) is not really tractable.

The resulting GIA uplift rates seem very smoothed...much more than the 100km smoothing constraint mentioned on p2004 ln17 would suggest. Please comment.
We think the reviewer is referring to p3005 line 17. Here we report the mesh density of the process to be on the order of 100 km (i.e. the side of the triangles in the triangulation are roughly 100km). This is not the length scale of the process, indeed the length scale needs to be much larger than this to be reconstructed from a 100 km mesh density. In this work we use 3000 km (p3004, ln13). This parameter was extracted from the Ivins and James (2005) GIA model.

A great deal of detail has been skipped regarding the methodology. The reader is not really left with a sense of how the whole system works. I realize you can't reproduce everything from earlier Zammit-Mangion et al paper, but I believe more can be done to describe the methodology. For example, the parameter layer isn't explained. And it's unclear how you go from the three layers to the FE mesh of the different processes to a final "statistically sound" result. How are you able to effectively separate the four different processes discussed in the Results section. Please consider adding some more explanation, figures, etc. in this section. At the moment, the methodology is very much a black box.
The reviewer is right in remarking that the methodology is detailed in the Zammit-Mangion paper. We have tried not to clutter the paper with too much mathematical detail but unfortunately this has made the analysis less clear in some areas. In the revised version we will expand Section 3, and include an overview diagram (similar to that in the paper of Zammit-Mangion et al.) to facilitate the understanding of this section.

Comparisons with ice core data is presented in support of the SMB results derived. Given the variability seen in the SEAT cores, it's difficult to accept any conclusions from the MEDLEY result, which represents just a few cores. What if the MEDLEY trend was an anomaly like SEAT 10-5? The Ligtenberg et al 2011 paper, which discusses the FDM derived using RACMO, made comparisons with 48 ice cores and looks to show good agreement with these cores. Many of these cores were in the WAIS, so there looks to be many other ice cores in the region that could be used to validate your model.
The reviewer addresses a valid point regarding the scarcity of ice core data for independent comparisons. Unfortunately, very few ice cores cover the observation period. In Ligtenberg's paper, the effects of firn compaction are addressed. This requires a larger observation period but it also allows for temporally cutting out a period of interest from the available data. Our comparison of a 7 year SMB anomaly trend is more dependent on perfect temporal agreement, and we did not have any other cores available for the 2003-2009 period. We will mention this in the revised version of the paper.

The abstract suggests it would be easily scalable for the whole of Antarctica. If so, then why was only the WAIS explored? All of the GIA/SMB/ice-mass change comparison studies (e.g., King et al, 2012, Shepherd et al, 2012, etc.) cover the AIS, so the same comparisons could be made. It would have made for a more complete comparison.
We agree with the reviewer that covering the whole of the AIS would have made it easier to better assess the performance of the framework. Unfortunately, as we hope the reviewer appreciates, the framework is computationally intensive (particularly in terms of memory) and at the time of writing we did not have the algorithms, nor the computational resources in place to consider the AIS as a whole. The study on the WAIS allowed us to explore computational tools to tackle this problem with ease, and establish a way forward. We are now implementing a similar approach for the entire AIS and that is why we know of the scaleability. We will alter the abstract to reflect this.

p2997, ln14: the Velicogna & Wahr is a bit dated, and their later papers show a lower proportion of GIA error. Consider updating reference.
We agree with the reviewer and will use more recent references (e.g. King et al, 2013, Sasgen et al 2014).

P2998, ln5: What if the SMB models have more than just systematic biases in them? For example, if the SMB variations themselves are modeled incorrectly (over/under estimated), then this would necessarily impact the spatial relationships used in the combination. This gets back to the earlier comment regarding the error analysis.
An advantage of the proposed approach is that any biases in the models, whether systematic or not, are not propagated to the framework. We use the models to extract typical length scales and orders of magnitudes; these are widely accepted to be correctly represented in the models. Biases would have affected our results if, for example, we had set the model output as the prior expectation of our process, which we do not. The amplitudes of inter-annual variability have been corroborated using independent estimates and we have confidence, therefore, that they are reproducing the correct of order of magnitude variability.

p3000, ln16: I assume these are formal errors on the trend. These tend to be optimistic, so I would recommend in the future applying some sort of error adjustment (bootstrapping, scaling, etc.) to make them more realistic.
This is an important point but it has not been tackled at this stage of the project. In fact, we have dealt with this problem in a recent paper by taking into account small-scale variations, and can include a sentence detailing this in an updated version of the paper.

p.3001, ln2: Considering you are using a RL04 GRACE mascon solution, which is a now dated release, it would have been very insightful to see how the results were affected when only the GRACE component was changed to, say, the CSR RL05 fields. In addition, how do the mascons relate to the FE mesh? The mascon discs won't be aligned with the mesh triangle boundaries, so how is this treated (if indeed it's even a problem)?
Our collaborators have only very recently, and thereby later than the rest of the community, pre-released a new version of their mascon solution. Given that this paper is only a proof-of-concept project, we will detail effect of the new release on the results in a forthcoming paper. To be clear, however, the Release versions referred to above are not relevant to the Goddard mascon solutions which are determined directly from the K band range-rate data. They have no relationship to CSR, JPL, GFZ or other spherical harmonic solutions. The most recent version of this mascon solution is version 2.

p3001, ln 20: The concern here is that the correlations would be more accurate if the mass loss was only due to surface mass changes, but a considerable amount of the observed mass change is related to GIA, which may have a different spatial signal. Plus, you're correlating mass variations using volume/height estimates. Most areas will have some correlation, but the degree of correlation will certainly vary, and introduce error. If this correlation between mascons is important, which I assume it is, it would be useful to see a more in-depth treatment of the error from the altimetry-based correlation, and its potential impact on the solution.
This relates to a query from referee 1. It is a non-trivial and important point which we will tackle in a forthcoming paper where we resolve the time varying component of the signals.

p.3001, ln23: What do you mean here by "averaging strength"?
Agreed that this is a bit unclear, we will modify the sentence to: "the extent of diffusivity is characterised by a parameter akin to the thermal coefficient in the heat equation, which is also estimated during inference (refer to Section 4.1 in Zammit-Mangion et al. for more details)."

p.3001, ln26: Should read "Thomas et al (2011)" instead of "Thomas and King (2011)". This occurs in other places as well.
Agreed, this will be corrected.

p.3006, ln9: It's not completely without prior information because the mass loss due to dynamics is constrained by the ice velocities described on p 3004, ln 16. This is equivalent to applying a type of forward modeling approach where all of the mass loss in essentially forced to go to regions of high velocity.
Yes and no! There is no one-to-one equivalence to a forward modeling approach; rather, it is only the probability for ice loss that is higher in areas with high ice velocity. We should stress that the framework does not "prevent" or disallow a dynamic signal in slow flow areas, it gives it a lower probability than in fast flow areas. Thus, for example, if GRACE detects a mass anomaly in a slow flow area with a length scale not characteristic of SMB (from altimetry) then it is possible to assign this to dynamics. In addition, in the time-evolving version of the framework, separation of SMB and dynamics will be improved because the former has, in general, high temporal variability, while the latter varies smoothly in time.

p.3007, ln25: If elastic effects are removed from the GPS displacements, wouldn't this impact your firn/elastic estimates?
In principle, the reviewer is correct. In this version of the framework however, the GPS stations are modeled to only measure GIA, therefore the elastic signal is removed in advance.

p3008, ln4: Why wasn't ICE-5G or the new ICE-6G included in the comparison analysis?
The key reason for this is that these are global solutions while the ones we compare to have been developed specifically for Antarctica. In addition, we wanted to include example of solutions derived from both forward modelling (W12a, IJ05-R2) and from data inversion (AGE-1, Gunter14).

p3008, ln 8: Isn't agreement with the GPS data nearly guaranteed since it is one of the input data sets?
This is an interesting point and it is worth mentioning. It is indeed not guaranteed, as the GPS data set is only one of several inputs (see comment above about data/solution misfits), and we are looking at a combination of these data. For example, in p2008 L10 we mention that there is poor agreement with the W06A station.

p3008, ln21: Wouldn't this agreement be mostly attributed to the smoothed nature of the RATES and AGE-1 solutions? Neither solution predicts GIA rates above 4mm/yr. Comparing a smoother solution to one with higher resolution and signal variation (W12a, IJ05-R2, and Gunter14) is an apples-to-oranges comparison, since they have different spectral content. Also, discussions of agreement should be done with uncertainties involved. Are the differences statistically significant? What are the uncertainties of the various components?

It is correct that we prescribe a certain spatial smoothness for the GIA solution. It is entirely possible that the real GIA signal is spatially less smooth than what we have assumed here. The degree of smoothness strongly depends on the "smoothness parameter" κ_{GIA} *mentioned above and the reviewer's comment highlights the fact that we have failed to state this clearly enough in the paper. However, the mean basin uplift rates should not, in our view, depend strongly on a higher resolution of the GIA field, so we cannot say that we agree with the conclusion that the agreement between AGE-1 and RATES is due only to the fact that they are both smooth solutions. Also, we believe that a basin comparison of uplift rates is a useful comparison for GIA models.*

p3012, ln5-25: It should be noted here that proper uncertainties of the input data sets is key towards generating reliable results. If, for example, the SMB estimates had 2-3cm uncertainties, then this would be reflected in the final estimate, i.e., the GIA rates would have large error bars. The same goes for the other data sets (altimetry, gravimetry, GPS). It's only a problem if the errors in the input data are too optimistic, i.e., lower than they are in truth.
Yes, this is correct. However, we ***do not*** *include any prior uncertainty estimates for SMB, only for the input data fields. Nonetheless, the referee is correct in stating that the solution is dependent on using the "proper uncertainties" and this is something that is surely a good thing! We would like to think that any reliable estimation would be dependent on the input errors. As stated earlier, we will detail our error estimation approach more fully in a revised m/s.*

p3012, ln26: The agreement with AGE-1 has been stated a couple of times, but when I visually compare the RATES and AGE-1 results, I don't see that much similarity, mainly because the RATES results have smoothed out most of the features. You might consider having a discrete color scale to better visualize the variations in Fig 7.
We do mention that the spatial pattern in RATES is different from that in AGE-1 (p3008 L8), but an updated figure can be included in the updated version of the paper to improve visualization.

Perhaps the station names can be added in one of the figures (e.g., Fig 8?).
We will include an updated figure.

Simultaneous solution for mass trends on the West Antarctic Ice Sheet

N.Schoen[1], A. Zammit-Mangion[1,2], ~~J.Bamber[1],~~ J. C. Rougier[2], T. Flament[3], F. Rémy[4], S. Luthcke[5], J. L. Bamber[1]

[1] {Bristol Glaciology Centre, School of Geographical Sciences, University of Bristol, UK}
[2] {Department of Mathematics, University of Bristol, UK}
[3] {School of Earth and Environment, University of Leeds, UK}
[4] {LEGOS, Toulouse, France}
[5] {NASA, Greenbelt, MD, USA}
Correspondence to: Jonathan Bamber (j.bamber@bristol.ac.uk)

Abstract

The Antarctic Ice Sheet is the largest potential source of future sea-level rise. Mass loss has been increasing over the last two decades ~~in~~ for the West Antarctic Ice Sheet (WAIS), but with significant discrepancies between estimates, especially for the Antarctic Peninsula. Most of these estimates utilise geophysical models to explicitly correct the observations for (unobserved) processes. Systematic errors in these models introduce biases in the results which are difficult to quantify. In this study, we provide a statistically rigorous, error-bounded trend estimate of ice mass loss over the WAIS from 2003–2009 which is almost entirely data-driven. Using altimetry, gravimetry, and GPS data in a hierarchical Bayesian framework, we derive spatial fields for ice mass change, surface mass balance, and glacial isostatic adjustment (GIA) without relying explicitly on forward models. The approach we use separates mass and height change contributions from different processes, ~~–~~ reproducing spatial features found in, for example, regional climate and GIA forward models, and provides an independent estimate, which can be used to validate and test the models. In addition, ~~full~~ spatial error estimates are derived for each field. The mass loss estimates we obtain are smaller than some recent results, with a time-averaged mean rate of -76 ± 15 GT/yr for the WAIS and Antarctic Peninsula (AP), including the major Antarctic Islands. The GIA estimate compares ~~very~~ well with results obtained from recent forward models (IJ05-R2) and ~~inversion~~ inverse methods (AGE-1). ~~Due to its computational efficiency, the method is sufficiently scalable~~The Bayesian framework is sufficiently flexible that it can, eventually, ~~to include~~ be used for the whole of Antarctica, can be adapted for other ice sheets and can ~~easily be adapted to assimilate~~utilise data from other sources such as ice cores, accumulation radar data and other measurements that contain information about any of the processes that are solved for.

1 Introduction

Changes in mass balance of the Antarctic ice sheet have profound implications on sea level. While there is a general consensus that West Antarctica has experienced ice loss over the past two

decades, the range of mass-balance estimates still differ~~s~~ significantly (compare, ~~e.g.~~for example, estimates in Shepherd et al. (2012), Tables S8 and S11 which range from -84±18 for GRACE to -13±39 Gt yr^{-1} for ICESat for the WAIS and from -24±35 to 123±60 for the East Antarctic Ice Sheet). ~~with Gunter et al. (2013)~~). Reconciling these disparate estimates is an important problem. ~~Studies~~ Previous studies have ~~typically make~~ made use of satellite altimetry (Zwally et al 2005~~Shepherd et al. (2012)~~), satellite gravimetry (Chen et al., 2006; King et al., 2012; Sasgen et al. 2013; Luthcke et al., 2013), or a combination of satellite and airborne data and climate model simulations (Rignot et al., 2011) to provide estimates. In the latter case, the balance is found by deducting output ice flux from input snowfall in a technique sometimes referred to as the Input-Output Method (IOM) or mass budget method.

Different approaches have different sources of error. ~~The dominant~~A key error in the gravimetry-based estimates is a result of incomplete knowledge on glacial isostatic adjustment (GIA), which constitutes a significant proportion of the mass-change signal but leakage and GRACE errors are also important (Horwath and Dietrich, 2009)~~{Horwath, 2009 #2174}~~(~~Velicogna and Wahr (2006)~~). For satellite altimetry, uncertainties arise from incomplete knowledge of the temporal variability in precipitation (Lenaerts et al.,2012, Frezzotti et al.,2012), and the compaction rates of firn (Arthern et al., 2010, Ligtenberg et al., 2011): quantities which play a ~~centre~~ central rôle in determining the density of the observed volume change. For the IOM, the main sources of errors stem from the surface mass balance (SMB) ~~profiles~~ estimates used (obtained from a regional climate model), and uncertainties in ~~the ice discharge map~~ice discharge across the grounding line. Recent improvements in regional climate modelling have reduced the uncertainty in the SMB component but differences between estimates for the Antarctic ice sheet as a whole still exceed recent estimates of its mass imbalance. For example, a recent update of the commonly used regional climate model, RACMO, has resulted in a change in the integrated ice sheet-wide SMB of about 105 Gt yr^{-1} (Van Wessem et al, 2014), which is larger than most recent estimates of the ice sheet imbalance. This change in SMB, directly impacts the IOM estimate by the same amount. It is these hard-to-constrain biases in the forward models, such as the one just described, that has, in part, motivated our approach.~~(Van den Broeke et al. (2006), King et al. (2012))~~.

~~To~~ In an attempt to ~~minimize~~ reduce the dependency on forward models, recent studies have combined altimetry and GRACE to obtain a data-driven estimate of GIA and ice loss simultaneously (Riva et al.,2009, Gunter et al.,2013). Here, we ~~aim to~~ extend these earlier approaches in a number of ways. We provide a model-independent estimate not only of GIA, but also of the SMB variations, firn compaction rates and of the mass loss/gain due to ice dynamics (henceforward simply referred to as ice dynamics). In doing so, we eliminate the dependency of the solution on solid-Earth and climate models. The trends for ice dynamics, SMB, GIA, and firn compaction are obtained independently through simultaneous inference in a hierarchical statistical framework. The climate and firn compaction forward models are used solely to provide prior information about the spatial smoothness of the SMB-related processes. Systematic biases in the models have, therefore, minimal impact on the solutions. In addition, we employ GPS bedrock uplift rates to further constrain the GIA signal. In future work the GPS data will also be used to constrain localised ice mass trends that cause an instantaneous elastic response of the lithosphere (Thomas and King (2011). The statistical framework uses expert knowledge about smoothness

properties of the different processes observed (i.e. their spatial and temporal variability) and provides statistically sound regional error estimates that take into account the uncertainties in the different observation techniques (Zammit-Mangion et al. 2014)~~{Zammit-Mangion, 2014 #2727}~~. The study reported here was performed as a proof-of-concept for a time-evolving version of the framework for the whole Antarctic ice sheet, which is currently under development. The time-evolving solution will use updated data sets and, as explained above, will also solve for the elastic signal in the GPS data. In addition, it will provide improved separation of the processes because of the additional information related to temporal smoothness that can be incorporated into the framework (discussed further in section 5).

~~The paper is organised as follows. In Section 2 we describe both the observation data and auxiliary data sets used while in Section 3 we give a summary of the statistical methodology employed (full details can be found in Zammit-Mangion et al. (2013)). Section 4 outlines the main results and is followed by a discussion in Section 5. Section 6 concludes the work.~~

2 Data

In this section we describe the data employed, which is divided into two groups. The first group contains observational data which play a direct rôle in ~~providing~~ constraining the mass ~~balance estimates~~trend. These include satellite altimetry, satellite gravimetry and GPS data (Sections 2.1–2.3). The second group ~~contains~~ comprises auxiliary data (both observational and data extracted from geophysical models), which we use to ~~aid the assimilation implicitly~~help with the signal separation (differentiating between the different processes we solve for accounting for their spatial smoothness) (Zammit-Mangion et al. 2014)~~{Zammit-Mangion, 2014 #2727}~~. These are discussed in Section 2.4.

2.1 Altimetry

We make use of two altimetry data sets in this study, obtained from the Ice, Cloud and land Elevation Satellite (ICESat) and the Environment Satellite (Envi~~S~~Sat).~~.~~

~~**ICESat:**~~ In this study, we used ICESat elevation rates (*dh/dt*) based on release 33 data from February 2003 until October 2009 (Zwally et al.,2011). The data includes the "86S" inter-campaign bias correction presented in Hofton et al., 2013) and the centroid Gaussian correction (Borsa et al., 2013) made available by the National Snow and Ice Data Centre ~~(NSIDC)~~. Pre-processing was carried out as described in Sørensen et al., 2011). Since ICESat tracks do not precisely overlap, a regression approach was used for trend extraction, in which both spatial slope (both across-track and along-track) and temporal slope (*dh/dt*) were simultaneously estimated (Howat et al., 2008), Moholdt et al., (2010). A regression was only performed if the area under consideration, typically 700m long and a few hundred metres wide, had at least 10 points from four different tracks that span at least a year. Regression was carried out twice, first to detect outliers (data points which lay outside the 2σ confidence interval), and second to provide a trend estimate following outlier omission. The standard error on the regression coefficient (in this case *dh/dt*), SE_{coef} , was calculated through (Yan (2009):

Formatted: Space Before: 12 pt

$$SE_{coef} = \frac{1}{\sqrt{n-2}} \sqrt{\frac{\sum_i e_i^2}{\sum_i (x_i - \bar{x})^2}} \quad (1)$$

where $\boldsymbol{e} = [e_i]$ is the vector of residuals, n is the sample size, and $\boldsymbol{x} = [x_i]$ is the input with mean $\overline{x}$. It should be noted that this standard error is not equivalent to the measurement error, but takes into account sample size, as well as the variance of both input data and residuals of the regression. Only elevation changes with an associated standard error on *dh/dt* of less than 0.40m/yr were considered. The 0.40m/yr threshold was selected by trial and error to avoid a noisy spatial pattern of points that are close together and opposite in sign, usually because the regression is based on a small subset of overpasses. Data above the latitude limit of 86° S were omitted. The remaining data were gridded on a polar-stereographic projection (central latitude 71°S; central longitude 0°W, and origin at the South Pole), at a 1 km resolution and then averaged over a 20km grid. The error used in the modelling framework was then the spread (standard deviation) of the trends within each 20km grid box, as in Riva et al., 2009).

~~**EnviSat:**~~ The Envis~~S~~at mission data began in September 2002 and ended in ~~November 2010~~April 2012. Compared to laser altimetry, radar altimetry is, in general, less suited for measurements over ice for several well-known reasons: the large spatial footprint, ~~–~~the relatively poor performance in steeper-sloping marginal areas (Thomas et al., 2008), and the variable snow-pack radar penetration ~~{Davis, 1996 #880~~(Davis, 1996)~~}~~. On the other hand Envis~~S~~at data exhibit better temporal and spatial coverage over much of the WAIS, primarily because of the instrument issues associated with ICESat that resulted in a shorter repeat cycle and less frequent operation than originally planned. We use the ~~EnviSat altimetry~~ along-track ~~trends~~ dh/dt trends presented in Flament et al., 2012), which were obtained by binning all points within a 500m radius and then fitting a 10-parameter least-squares model in order to simultaneously correct for across-track topography ~~and~~, changes in snowpack properties and dh/dt. The re-trended residuals were then used to obtain linear trends over the 2003–2009 ICESat period for our study. As with ICESat, the data were averaged over a 20km grid and the standard deviation of the trends were used as the error at this scale.

2.2 GRACE

The Gravity Recovery and Climate Experiment (GRACE, Tapley et al., 2005) has provided temporally continuous gravity field data since 2002. Different methods have been used to provide mass change anomalies from the Level 1 data. Most are based on the expansion of the Earth's gravity field into spherical harmonics; but to make the data usable for ice mass change estimates, it is generally necessary to employ further processing methods. These include the use of averaging kernels (Velicogna et al., 2006), inverse modelling (Wouters et al., 2008), Sasgen et al., 2013), and mass concentration (mascon) approaches ~~–~~(Luthcke et al., 2008)~~{Luthcke, 2008 #2127}~~. Spherical harmonic solutions usually depend on filtering to remove stripes caused by correlated errors (Kusche et al., 2009), Werth et al., 2009).

In this paper, we used ~~the latest~~a ~~release of mascon solutions (Luthcke et al., 2013), although we stress that the presented~~ framework is not limited to this class of solutions. The mascon approach employed here directly uses the GRACE K-band inter-satellite range-rate (KBRR) data which are

then binned and regularized using smoothness constraints. The release 4 (RL4) Atmosphere/ Ocean model correction, which utilizes the European Centre for Medium-Range Weather Forecasts ~~(ECMWF)~~ atmospheric data and the Ocean Model for Circulation and Tides (OMCT), was used (Dobslaw and Thomas (2007). Some concerns with this correction have been reported (Barletta et al., 2012), but a release of the mascon data using the corrected version (Dobslaw et al., ~~(~~2013) ~~is not yet~~was not available for this study. Contributions to degree-one coefficients were provided using the approach by Swenson et al., 2008). The mascon approach used here does not call for a replacement of C20 coefficients. We assume that GRACE does not observe SMB or ice mass changes over the floating ice shelves as they are in hydrostatic equilibrium). Hence, all observed mass changes over the ice shelves are assumed to be caused by GIA.

Although the mascons are provided at a resolution of about 110km, their fundamental resolution is ~~very~~ nearer that of the original KBRR data ~~itself~~ (~300km, Luthcke et al., 2013). For the statistical framework, it is important to quantify the correlation among the mascons so that it is taken into account when inferring both the processes and associated uncertainties. We quantify the spatial correlation by determining an averaging model such that the diffused signal is able to loosely reconstruct the mass loss obtained using only altimetry (and assuming that all height change occurs at the density of ice). The averaging strength between mascon neighbours is also estimated during the inference (Zammit-Mangion et al., ~~(~~20143). The error on the mascon rates is assumed to be a factor of the regression ~~errors~~residuals on the trends, ~~which is also estimated~~in a similar manner to the altimeter data ~~({Zammit-Mangion, 2014 #2727}ibid.~~ (Zammit-Mangion et al. 2014)The a-priori errors, after these two steps, are shown in Figure 1, which also indicates the length-scale over which we estimated the GRACE mascons to be uncorrelated. ~~.~~

2.3 GPS

The GPS trends used in this work were taken from Thomas and King (2011). Not all of the trends were suitable for our analysis, as the ~~record~~ length of record did not always coincide with the 2003–2009 ICESat period. We only used stations with contemporaneous data, as well as those where we could access the original time series to confirm that the trend had stayed the same, within the error bounds, for our observation period. For the North Antarctic Peninsula, we followed the approach suggested in ~~the~~ Thomas and King (2011) and used the pre-2003 trends, ignoring the later trend estimates which are ~~highly contaminated~~strongly influenced by elastic signals. All other stations were corrected for elastic rebound as in Thomas & King (2011) and subsequently assumed to be measuring GIA only (the published rates were used). A more ~~sophisticated~~ advanced approach where the estimated ice loss is fed back into a dynamic estimate of the elastic rebound, is being implemented for a spatiotemporal extension of ~~this work~~the Bayesian framework. The GPS data used in this study are ~~compiled~~ detailed in Table 1.

2.4 Additional data sets

RACMO.~~:~~ Elements of the Regional Atmospheric Climate Model version 2.1 (RACMO, Lenaerts et al., 2012) were used to constrain SMB properties. Spatially-varying length scales describing spatial smoothness of precipitation patterns were obtained from the 2003–2009 SMB anomalies (with respect to the 1979–2002 mean). These ranged from 80km in the Antarctic Peninsula to

200km east of Pine Island Glacier. The amplitude of the anomalies, which peaked at ~~50mmweq~~ 50 mm water equivalent in the Antarctic Peninsula, was used to ~~extract~~ provide the order~~s~~ of magnitude annual amplitudes for expected regional SMB ~~estimates~~variability (Zammit-Mangion et al. 2014)~~{Zammit-Mangion, 2014 #2727}. See Zammit-Mangion~~ et al., ~~2013) for details~~. RACMO2.1 also provides a surface density map: the mean annual density of the surface layer. This was used to translate height changes corresponding to the SMB field to mass changes.

Firn correction.~~:~~ We used the firn correction anomalies for 2003–2009 (with respect to the 1979–2002 mean) from a firn compaction model (Ligtenberg et al., 2011). These anomalies were used to estimate, empirically, the correlation between firn compaction rate and surface mass balance. This relationship was then subsequently used to determine jointly the SMB and firn correction processes, subject to the constraint that firn compaction is a linear function of SMB (supported by the high correlation between the respective 2003–2009 trends). The methodology automatically takes into account inflated uncertainties due to confounding of these two processes (since they have identical length scales), (Zammit-Mangion et al. 2014)~~{Zammit-Mangion, 2014 #2727}~~.

Ice Velocities.~~:~~ We use surface ice velocities derived from Interferometric Synthetic Aperture Radar (InSAR, Rignot (2011) data. In places where no observational data were available, theoretical balance velocities (Bamber (2000) were used. ~~Ice velocities were used~~This composite velocity field was employed to help~~ constrain the amount of potential height change which can be attributed to~~ in the separation of signals due ice dynamics versus those due to SMB (Section 3).

3 Methodology

Our statistical framework makes use of several recent improvements in statistical modelling which can be exploited for geophysical purposes. Complete d~~D~~etails reagarding the mathematical methods employed are given in ~~(~~Zammit-Mangion et al., 2014~~3~~) and~~;~~ here, we ~~only give a brief~~provide a conceptual overview of the approach. A description of the software implementation can also be found in Zammit et al, (2015). The statistical framework hinges on the use of a hierarchical model where the hierarchy consists of three layers, the observation layer (which describes the relation of the observations to the measured fields), the process layer (which contains prior beliefs of the fields using auxiliary data sets) and the parameter layer (where prior beliefs over unknown parameters are described).

The 'observation model' is the probabilistic relationship between the observed values and the height change of the each of the processes. For point-wise observations, such as altimetry and GPS, the observations were assumed to be measuring the height trend at a specific location. GRACE mascons, on the other hand, were assumed to represent integrated mass change over a given area. These mass changes were translated into height changes via density assumptions: upper mantle density was fixed at 3800 kg/m^3; ice density at 917 kg/m^3, and SMB at values ranging from 350-600 kg/m^3. Recall (Section 2.4) that we used the density map from Ligtenberg et al., 2011) to specify the density of the surface layer.

In the 'process model' four fields (or latent processes) are ~~described~~modelled: ice dynamics, SMB, GIA, and a field which combines the processes which ~~do~~ result in height changes, but no mass changes: firn compaction and elastic rebound. We model the height changes due to these as

spatial Gaussian processes, i.e. we assume that they can be fully characterised by a mean function and a covariance function. For each field we assume that the mean function is zero (we do not use numerical models to inform the overall mean) and that the covariance function, which describes how points in space covary, is highly informed by numerical models and expert knowledge as described next. The relationship between the observations, priors and the latent process, defined by the process model is shown schematically in Figure 2. Those processes that are influenced by an observation are linked by a solid arrow and it is evident that the problem is underdetermined as there are less independent observations than there are latent processes. This is why the use of priors is important and useful for source separation (i.e. for partitioning elevation change between the four latent processes shown in Figure 2). It should also be noted that SMB and firn compaction have been assumed, in this implementation of the framework, to covary *a priori*, as discussed later.

The practical spatial range of surface processes – this describes the distance beyond which the correlation drops to under 10% – was estimated from RACMO2.1 as described in Section 2.4. This analysis revealed, for example, that locations at 100km are virtually uncorrelated in the Antarctic Peninsula, but highly correlated East of Thwaites. Similarly GIA was found to have a large practical range (~3000 km), from an analysis of the IJ05-~~R2~~ R1 model (although version R2 is used for comparison in the results and discussion) (~~Ivins~~ et al., ~~2013~~). These length scales impose soft restrictions on the possible class of solutions for the individual fields. They are useful, however, for helping to partition a height change between the different processes that can cause that change. For example, a long wavelength variation in height that spans different basins is likely associated with SMB, whereas a localised change that shows some relationship to surface velocity is likely associated with ice dynamics (Hurkmans et al., 2014).

~~Mass~~ Hence, mass loss due to ice dynamics was assumed to mostly take place in areas of ~~high ice velocity~~faster flow (Hurkmans et al., 2014). A "soft" constraint was thus placed on elevation rates due to ice dynamics such that it is small (1mm/yr) at areas of low velocities and ~~possibly~~ can be large (up to 15m/yr) at velocities greater than 10m/yr. A sigmoid function was used to describe this soft constraint:

$$\sigma_{vel}(s) = \frac{15}{1+exp(-(v(s)-10))} \quad (2)$$

where $v(\boldsymbol{s})$ denotes the horizontal velocity at location $\boldsymbol{s}$. For illustration of how $\sigma_{vel}(\boldsymbol{s})$ is used, an altimetry elevation trend of 10m/yr in Pine Island Glacier where velocities exceed 4 km/yr is within the $1\sigma_{vel}$ interval and thus classified as "probable". On the other hand, a 10m/yr trend in a region east of Thwaites, where velocities are 2m/yr, would lie within the $2000\sigma_{vel}$ level and thus assumed to be a virtually impossible occurrence *a priori*. At Kamb ice stream, this assumption had to be ~~altered~~ relaxed as this area shows thickening from the ~~stalling~~ shutdown of ~~ice stream C~~Kamb ice Stream about 150 years ago (Retzlaff and Bentley, 1993). Although the velocity of the ice is low, the thickening occurs at ~~comparably~~ relatively high rates. To reflect this, we fix $\sigma_{vel}(\boldsymbol{s})$ = 2m/yr in this drainage basin. In Table 2, we outline the key length-scale and amplitude constraints placed on the fields that are solved for in the framework. These soft constraints should be seen as ones characterising the solution in the absence of strong evidence to anything

Formatted: Font: Italic

otherwise. They can be 'violated' if the data is sufficiently informative. In the Discussion we examine the sensitivity of the solution to these constraints.

Length scales and prior soft constraints are easily defined for Gaussian processes (or Gaussian fields) which, on the other hand, are also computationally challenging to use. Gaussian fields can however be re-expressed as Gaussian Markov Random Fields (GMRF) by recognising that Gaussian fields are in fact solutions to a class of Stochastic Partial Differential Equations (SPDEs, Lindgren et al., 2011). Numerical methods for partial differential equations, namely, finite element (FE) methods, can thus be applied to the SPDEs in order to obtain a computationally efficient formulation of a complex statistical problem (Zammit-Mangion et al., 2014)~~{Zammit-Mangion, 2014 #2727}~~. Spatially varying triangulations (meshes) are used for the different processes reflecting the assumption that, for example, ice loss is more likely to occur ~~on~~ at smaller scales ~~on~~ near the margins of the ice sheet where fast, narrow ice streams are prevalent, than in the interior. We thus use a fine mesh at the margins (25km) and a coarse mesh in the interior for this field. GIA on the other hand is ~~a pre-supposed~~assumed to be smooth. This allows us to use a relatively coarse mesh for this process (~100km).

We note that ~~the~~ our methodology differs from others in that it is not an ~~simple~~ unweighted average of estimates with markedly different errors (Shepherd et al., 2012) or a sum of corrected data sources (Riva et al., 2009), but a ~~statistically sound,~~ process-based estimate. For each of the four fields (noting that elastic rebound and firn compaction covary in this implementation), we infer a probability distribution and standard deviation for every point in space. By relating pre-inference and post-inference variances, it is possible to assess the influence of different kinds of observation at each point on the resulting fields.

4 Results

Inferential results are available for ~~all~~ of the ~~four~~ three processes shown in Figure 2 in isolation. In this section we report the results for each of the processes in turn, ~~a discussion of these results is provided in Section 5~~but emphasise that these are presented to demonstrate the methodology rather than provide final estimates. This is because, as stated in section 2, improvements are planned both to the framework and the data sets that we use in it. In all the examples shown, green stippling indicates where the signal is greater than marginal standard deviation.

Ice dynamics.~~:~~ We obtain an ice dynamics imbalance of -86.25 ± 16.12 Gt/yr. The results for ice dynamics (Fig. 3~~1~~a) are consistent with prior knowledge of disequilibria in ice ~~dynamics~~ flow in the West Antarctic Ice Sheet (WAIS), for example, the ice build-up in the Kamb Ice Stream catchment (Retzlaff and Bentley, 1993) and the ~~rapid ice loss~~wastage in the Amundsen Sea Embayment (~~ASE,~~ Flament et al., 2012). The strength of the approach is apparent when focusing on the Antarctic Peninsula (Fig. 3~~1~~b). Due to the relatively narrow, steep terrain, and northern latitude (which affects the across track spacing of the altimetry) satellite altimeter data are sparse, while GRACE data are strongly affected by leakage effects, making it challenging to localise the mass sources and sinks. W~~ithout prior instruction, the~~e find that the framework places ice loss maxima at the outlets of several glaciers and ice streams, which are known to have accelerated ~~(De Angelis, 2003 #1531)~~(De Angelis and Skvarca, 2003). The result is a high-resolution map of

ice mass loss or gain that can be linked to specific catchments. Strong ice loss can be observed on the Northern Peninsula at the Weddell Sea shore, at the former tributaries of the Larsen B ice shelf. The maximum ice loss rate is found in the area around Sjögren Glacier with -4.7m/yr. Neighbouring Röhss Glacier, on James Ross Island, has been thinning considerably since the break-up of the Prince Gustav Ice Shelf (Glasser et al. 2011, Davies et al. 2011). This is also reflected in high loss rates. Hektoria and Evans, Gregory Glacier, and glaciers the Philippi Rise also show strong ice mass loss signals, most likely as a result of the collapse of the Larsen B ice shelf (Scambos et al., 2004, Berthier et al., 2012). Other ice loss maxima are found in the region of the Wordie Ice Shelf (see Fig. ~~8~~ 10 for reference), Marguerite Bay, and Loubet Coast, which corroborates findings from USGS/BAS and ASTER airborne stereo imagery analyses (Kunz et al., 2012). Ice loss is also observed on King George Island, which is in agreement with recent analyses of satellite SAR data (Osmanoğlu et al., 2013), and on Joinville Island. Ice build-up is observed over the Southern Peninsula (Kunz et al., 2012).

The gap in altimeter data around the pole results in spurious estimates for that region and the shaded area, south of 86°, is not considered here. As expected, the marginal standard deviation, or error estimate, (Fig. 4~~2~~) is lowest in the interior of the WAIS, where sampling density by altimetry is high, and highest on the Peninsula, where data are sparse. Also, steep coastal areas show larger errors, reflecting the dependency of altimeter errors on slope (see Bamber et al., 2005) or Brenner et al., 2007).

SMB and firn compaction~~:~~. We obtain an SMB imbalance of 10.57 ± 4.98 Gt/yr. Fig. 5~~3~~ shows the trend of the cumulative SMB anomalies according to RACMO 2.1, calculated with respect to the 1979–2010 mean. This approximately corresponds to the signal we are estimating, since we are only considering trends with respect to a ~~balance~~ steady state SMB. A cursory inspection of the anomalies we obtain (Fig 6) with those from RACMO2.1 (Fig 5) suggests relatively poor agreement. It should be noted, however, that the anomalies over the seven year interval are on the order of a few centimetres a year and only a limited area has a statistically significant trend in our inversion (stippled regions in Fig 6). There is a difference in sign between the model and our inversion for the Northern Antarctic Peninsula but again, the rates we obtain are below a significant threshold and the Peninsula possesses larger uncertainties than other areas for both our framework and the regional climate model. ~~The results we obtain for SMB (Fig. 4) largely differ from those of RACMO (Fig. 3). This holds especially for the Amundsen Sea Sector. Here, RACMO shows an overall positive trend while our estimate shows a localized negative trend inland, which follows the orography.~~ In Fig. 7~~5~~, we compare our results with ice core trends from Medley et al. (2013) who conclude that, while in phase, RACMO2.1 appears to show exaggerated inter-annual variability in the ~~ASE~~Amundsen Sea Sector. The ~~shown~~ ice core trend ~~titled~~ labeled 'MEDLEY' is the mean of ~~the~~ three ~~2010~~ cores PIG2010, THWAITES2010, and DIV2010 collected in 2010; the location in ~~the~~ Fig. 7 is, consequently, the mean ~~of the three cores'~~ coordinates for all the cores. The trends at the single ice cores were not listed, but ~~we can see~~there appears to be qualitative agreement with our negative trend in the area. Burgener et al. (2013) also provide new ice core records for the Amundsen Sea sector (Satellite Era Accumulation Traverse, SEAT) and Fig. ~~5~~ 7 also shows a comparison with their data. Trends were taken over the full 2003–2009 period relative to~~;~~ ~~the~~ a mean ~~is~~ for 1980-2009. The agreement is good for three out of

Formatted: Font: Not Bold

five cores given in the paper. Following Burgener et al. (2013), we exclude SEAT 10-4 because of the high noise level in the isotope dating and surface undulations. SEAT10-5 shows a relatively strong negative trend that ~~cannot~~ we do not ~~be~~ reproduce~~d~~. SEAT-01, SEAT-03, and SEAT-06 agree well with our results at ~~a centimetre scale~~the ± cm yr^{-1} level. We note, however, that there is ~~relatively large~~substantial short-wavelength spatial variability in SMB based on the ice core data, which is below the resolution ~~not catered for in~~of our framework. This also suggests that a single ice core measurement should be treated with caution in this type of comparison.

Height changes from firn compaction and elastic rebound are estimated together in ~~one~~ a single field. Because they take place on similar length scales, and there is no temporal evolution in ~~the~~ our time-invariant solution presented here, they are confounded in this study. Since firn compaction occurs at relatively large rates (cm a^{-1}), we cannot make any useful inferences about elastic rebound rates. We expect this issue to be less critical in the time-evolving ~~solution~~version of the framework. The modelled inverse correlation between firn compaction and SMB (Section 2.4) is visible in the results (Fig. ~~6~~4 and Fig. ~~8~~6).

GIA.~~:~~ We obtain a GIA rate that is equivalent to a mass trend of 12.34 ± 4.32 Gt/yr. It is difficult to compare this directly with other published results because the domain is not the same. We do, however, examine individual basins. The GIA vertical velocities estimated by our framework are ~~considerably~~ lower than ~~many~~ some older forward model solutions (e.g. Peltier (2004), Ivins and James (2005). Our results, however, agree well with a recent GRACE-derived estimate, AGE-1, which also ~~adopts the assumption~~assumes that over the ice shelves, GIA is the sole process causing observed mass change (Sasgen et al., 2013). Compared with AGE-I, our maxima in vertical uplift are shifted towards the open ocean for both of the major ice shelves (Fig. ~~7~~9). Agreement with the trends at most GPS stations is good; however, the imposed smoothness constraints have a larger influence. The W06A station (Table 1), which has a strong negative trend with a large error, exacerbated by a strong elastic signal, stands out. Thomas and King (2011) show that its rate does not fit with any of the GIA models used in their comparison. The signal is effectively ignored in ~~this~~ our framework due to the large spatial scale assumed for the GIA process.

In Fig. ~~9~~12, we compare our results (denoted 'RATES') with basin estimates from AGE-1 (Sasgen et al., 2013), two recent forward models, W12a (Whitehouse et al., 2012) and IJ05-R2 (Ivins et al., 2013), and a data-driven inversion by Gunter et al. (2013) (denoted 'Gunter13'), which is an update of Riva et al. (2009). Basin definitions are shown in Fig. ~~8~~11. Both Gunter13 and AGE-1 rely on GRACE data. W12a, while a forward model, was adjusted to better match GPS uplift rates on the Peninsula. ~~Overall~~In general, over the domain covered in this study, we obtain ~~best~~ closest agreement with the AGE-1 solution. For the Filchner Ronne Ice Shelf (basin 1), the AGE-1 estimate (2.1 mm/yr) is slightly lower than ours (2.7 mm/yr), while IJ05-2 is slightly higher (3.5 mm/yr). W12a (7.2 mm/yr) shows more than twice our rate in this area, while Gunter13 (4.2 mm/yr) lies between IJ05-R2 and W12a. At the Ross Ice Shelf (basin 18), the agreement with AGE-1 and IJ05-R2 (both 1.9 mm/yr, RATES 2.0 mm/yr) is very close. Gunter13 (3.1 mm/yr) and W12a (3.4 mm/yr) are slightly higher. For basin 19, again the agreement with AGE-1 and IJ05-R2 is close with RATES at 2 mm/yr, AGE-1 at1.7 mm/yr and IJ05-R2 at (1.9

mm/yr). Gunter13 and W12a are, again, somewhat higher here, at 2.6 mm/yr and 2.7 mm/yr, respectively. All model estimates lie within our error bounds.

Basin 20 lies between the Ross Ice Shelf region and the Amundsen Sea sector. Here, our uplift rate (1.1 mm/yr) ~~agrees best with~~lie closest to IJ05-2 (0.9 mm/yr), with AGE-1 at 0.5 mm/yr and W12a at 1.8 mm/yr. Gunter13 has the highest rate (2.2 mm/yr) for this basin. Basins 21 and 22 extend to the Amundsen Seas Sector, one of the most rapidly changing areas in Antarctica. The large volume of ice loss in this area causes large elastic loading responses. Groh et al. (2012) and Gunter et al. (2013) have both mentioned the possibility of a present-day viscoelastic signal in this area. Our uplift estimate for basin 21 is comparably small at 0.6mm/yr. AGE-1 (0.7 mm/yr) is closest to this estimate, while IJ05 (1.6 mm/yr) and W12a (3.1 mm/yr) are considerably higher. Gunter13 has the highest rate at 5.4mm/yr. In basin 22, again, we agree best with AGE-1 (1.1mm/yr, RATES at 0.9 mm/yr), while all other estimates are higher. Gunter and W12a cover the higher end at 4.5 mm/yr and 4.8 mm/yr respectively, and IJ05-R2 lies in the middle at 3.0 mm/yr. Basin 23, which connects the ASE to the Southern Peninsula, also yields a small uplift rate (0.4mm/yr). AGE-1 (0.5mm/yr) lies within the error estimate, with IJ05-R2 (1.7mm/yr) and Gunter13 (2.0mm/yr) just outside, and W12a considerably higher at 5 mm/yr.

On the Southern Peninsula (basin 24), agreement with AGE-1 (1.2 mm/yr, RATES 1.3 mm/yr) is very good, but W12a is close (1.8 mm/yr). Gunter13 and IJ05 both show uplift on the Southern Peninsula, but at a higher rate of 2.4 mm/yr and 3.1 mm/yr, respectively. On the Northern Peninsula, again the agreement is best with AGE-1 (0.8 mm/yr, RATES 0.7 mm/yr), followed by IJ05-R2 (0.5 mm/yr). The W12a rate is higher at 1.7 mm/yr. Gunter13 is the only model that shows a negative GIA trend (-0.70 mm/yr) in this region.

5 Discussion

In Fig. ~~10~~ 13 and Table 3~~2~~ ~~show~~ we present the basin-scale combined ice and SMB loss in comparison with two recent studies using GRACE (King et al., 2012), Sasgen et al., 2013). The ~~Sasgen et al. (2013)~~latter study ~~rates~~ spans the ICESat period and the rates were derived for this publication. The ~~King et al. (2012) rates~~former study, however, spans the 2002–2010 period. Basin definitions are the same as those in Sasgen et al. (2013) (as shown in Fig. 11~~8~~) but differ from King et al. (2012): the sum of our basins 1 and 24 match the sum of their basins 1, 24 and 27. Our basin 25 matches the sum of their basins 25 and 26. Consequently, comparisons for these basins are not shown in Fig. 13~~0~~ but provided in Table 3~~2~~.

Overall, ~~the~~ we obtain good agreement with Sasgen et al. (2013)~~ is close: we arrive at a~~. Our mean, time-averaged ice loss rate of -76 ± 15 GT/yr, ~~compared with~~deviates by less than one standard deviation from the value of -87 ± 10 GT/yr ~~for~~ obtained by Sasgen et al. (2013). Agreement at the basin scale is also good. For Basin 18, our error estimates are inflated because of the pole gap in the altimetry data. The largest differences occur in basins 19, 20 and 23. For 19 and 20, agreement is very good when comparing the sums of the two adjacent basins – ~~indicating~~ suggesting that leakage effects might be ~~playing a key rôle~~affecting ~~in this~~the ~~discrepancy (due to the particular geometry of the basins)~~ability of a GRACE-only solution to fully isolate the signal to each basin. For basin 23, the altimetry – both EnviSat and ICESat – show a clear positive trend

in this area (ICESat: +4 GT/yr), with only very localized ice loss signals on Ferrigno ice stream. This positive trend (as opposed to a negative trend from GRACE) reduces the ice loss estimate and causes the ~~discrepancy~~difference between the two estimates. The strong GRACE mass loss signal for the Amundsen Sea sector leads to increased leakage in the coastal basins. The King et al. (2012) result shows basins 23 and 21 are strongly correlated at p=0.96. When comparing the sum over the coastal basins 21, 22, and 23, the difference between the Sasgen et al. (2013) estimate (-80 GT/yr) and ours (-74 GT/yr) reduces to ~~just~~ 6 GT/yr.

We also compare our basin scale results to ice loss rates from King et al. (2012). Here, the observation periods ~~do not coincide~~are not identical, and the GIA estimates differ ~~widely~~. Still, there is ~~reasonable~~ generally good agreement at the basin-scale, in particular, ~~. Good agreement is observed in basins~~ where their GIA estimates (Whitehouse et al., 2012) lie within our error ranges (basins 18, 19) and worst where their GIA uplift rate is a multiple of ours (sum of basins 1 and 24). Overall, their ice loss rate of -118 ± 9 GT/yr is significantly higher than ours.

~~Overall~~Integrated over the domain studied, our loss estimate is lower than other ~~current~~ recent estimates: Shepherd et al. (2012) arrive at -97 ± 20 G~~t~~T/yr for WAIS over the ICESat period; while Gunter et al. (2013) obtain -105 ± 22 G~~t~~T/yr. With regards to Shepherd et al. (2012) and other altimetry-based results, the discrepancy is ~~mostly due to~~partly explained by our estimate of a negative SMB anomaly in the ASE, while~~.~~ RACMO2.1 gives a positive ~~signal~~ trend in this region (Fig. ~~3~~5). Methodologies employing RACMO2.1 will, ~~hence~~thus, attribute a greater loss (for a given height change) to ice dynamics. Since these losses occur at a higher density than SMB, the ~~induced~~ inferred mass loss is greater. With regards to Gunter et al. (2013), the discrepancy arises from the different ~~estimated~~ GIA rates used in the ASE. One cause for this might be the different GRACE solutions used. Our GRACE data set (Luthcke et al., 2013) is equivalent to a RL04 GRACE solution and uses the same antialiasing products. In Gunter et al. (2013), RL05 GRACE solutions appear to yield higher overall mass loss estimates. ~~Still, p~~Preliminary comparisons of new (RL05) mascon solutions with the RL04 ones appear to show, however, little impact on the trends. ~~A study of the influence of the different GRACE solutions, which would encompass different releases and include a comparison between spherical harmonics and mascon solutions is noted as future work.~~

The results for SMB ~~stand out in this study as they do not agree with those obtained from RACMO (Lenaerts et al. (2011))~~are more challenging to interpret because the trend, over this time period, is relatively small (a few cm/yr) and below one standard deviation for most of the domain (Fig 6). ~~However~~There is, however, some agreement ~~can be shown~~ with new *in-situ* data from ~~deep~~ ice cores (Medley et al., 2013~~);~~, Burgener et al., 2013). It should be remarked that in the ~~Amundsen Sea Embayment~~ASE, where we also observe an ice loss maximum, the statistical framework might have difficulty in ~~separating~~ partitioning SMB and ice dynamics. The reason for this is that the density of the SMB changes tends to be higher at the coast, with higher temperatures and melt rates. Some of the large, negative trends seen in the ASE could thus be falsely attributed to SMB. This could be remedied in principle by including more information on the spatial patterns of SMB into our framework by using, for example, a more informative prior. Also, it should be noted that the uncertainties on our SMB rates, although low on a basin scale, are ~~comparably~~ comparatively high on a small spatial scale. These issues will become less critical in a

Formatted: Font: Italic

time-evolving solution because ice dynamics and SMB have very different temporal frequencies: the former tends to vary smoothly in time, while the latter has relatively large high-frequency variability. This important difference in temporal smoothness will elicit significant improvement in source separation. ~~This is in part an intrinsic problem in signal separation, but could be improved by adding in-situ data which was used for validation in this analysis.~~

Methods that combine altimetry and gravimetry such as Gunter et al. (2013) and ~~also this paper are very sensitive to differing SMB estimates~~also the framework presented here are sensitive to the SMB anomaly used. We illustrate this sensitivity ~~in~~ through a simple calculation: ~~L~~let the unobserved ~~reality~~ processes on a 1 m^2 unit area be as follows: SMB amounts to 0.2 m/yr at 350 kg/m^3 density; GIA is 1 mm/yr at 3500 kg/m^3; and ice loss is at -1.0 m/yr at ~~971kg~~917 kg/m^3. This amounts to an observed height change of -0.799 m/yr. The observed mass change is -897.5 kg/yr ~~on~~ over the unit ~~m~~^{2}area. We now try to explain these signals by taking into account GRACE and altimetry, but erroneously assume ~~an~~ a SMB rate that is ~~slightly~~ 10% too high ~~2cm higher~~ at 0.22m/yr (amounting to a positive mass change of 77 kg/yr). The remaining mass signal that needs to be explained by ice and GIA is now -974.5 kg/yr. The unexplained height change is -1.019 m. We arrive at two equations, one for height and one for mass, that can be solved by finding the intersection of the two lines (see Fig. ~~11~~14). Solving the equations, we arrive at an ice mass loss rate of -1.025 m/yr with a high, but still plausible, GIA rate of 6 mm/yr. ~~So overall~~Thus, ~~a 2cm~~in this example, a 10% difference in SMB can result in a GIA estimate that is ~~considerably~~ markedly higher (5 mm/yr) than the truth. The resulting ice mass difference would be in the range of -40 ~~GT~~ Gt/yr when taken over the whole of West Antarctica. Naturally, this sensitivity acts both ways, so an underestimate ~~of~~ in SMB would result in a lower GIA, and ~~lower~~ less ice loss. In this context, both GRACE filtering and the treatment of the ICESat trends also play a major rôle. As the mass loss signal in ~~this region is very local~~West Antarctica is highly localised, with ~~very~~ high rates of elevation change confined to ~~several kilometres~~only a few percent of the area of a basin, the inclusion or exclusion of a single (informative) ~~pixel in the~~ altimetry data point can alter the ~~height change signal~~spatial distribution of height change considerably but less, the overall mass trend, as this is constrained by GRACE.~~.~~

It is also worth examining the sensitivity of the solution to the prior distributions that were derived from the forward models, auxiliary data sets, such as surface ice velocity, and expert knowledge. To do this, we changed the original amplitude and length-scale constraints as detailed in Table 4. The Table also lists the original mass trend (using constraints detailed in Table 2) alongside the new estimates using the revised constraints. Changes in the characteristic length scale for GIA and SMB have a rather small effect on the integrated mass trend. On the other hand, the velocity threshold that is used to determine whether the signal is likely to be associated with ice dynamics appears to have a significant effect for the three basins that comprise the Antarctic Peninsula: 23, 24, 25. This is because, for the Peninsula, observed and balance velocities are missing in a number of places. Where this is the case, they were set to 5 m/yr. With a 50 m/yr soft threshold this means that an ice dynamics signal is extremely unlikely in all locations with a missing velocity. Improving the velocity field in this area would, therefore, reduce this sensitivity.

The GIA estimates from our study agree ~~very~~ well with a recent GRACE-based estimate (Sasgen et al., 2013) and also compare well ~~to state-of-the-art~~with a recent forward model (Ivins et al.,

2013). Compared to AGE-1, the spatial pattern of our uplift maximum is shifted away from the Peninsula and towards the Ronne Ice Shelf. The spatial pattern ~~resembles more the~~is closer to that of W12a and ICE-5G models, with a bimodal uplift maximum centred underneath the Ronne and Ross Ice Shelves (Fig 9). This spatial structure is likely to have resulted from the use of GPS uplift rates, which were also used in the calibration of the most recent forward models (Whitehouse et al., 2012), Ivins et al., 2013). The W12a model yields slightly higher estimates for most basins but shows good agreement ~~in~~ on the Southern Antarctic Peninsula. Whitehouse et al. (2012) remark that the uplift rates using the W12 de-glaciation history – which are already substantially lower than the ICE-5G (Peltier 2004) model rates – can be viewed as an upper bound. ~~In this light, our estimates corroborate the general shift in expert opinion in recent years towards a lower GIA uplift rate. However, note that all the above-mentioned GIA estimates share common data – IJ05-R2 uses geological data collated by Whitehouse et al. (2012); which in turn uses the same GPS data (Thomas and King (2011)) that is used by Sasgen et al. (2013) and also in this study. While the lower rates agree better with IJ05-R2 and AGE-1, the spatial pattern of the uplift conforms better with that of W12a, or ICE-5G. It should be remarked that, although we used some common GPS trends which were also employed in the adjustment of W12a, we only used a subset of the Thomas and King (2011) data set because not all time series were available for the 2003–2009 time period at the time of writing (See Table 1, Fig. 7) .~~

Separating secular and present-day viscous and elastic signals from the trends in this area remains a challenging task and will be treated in greater detail in the spatio-temporal version of our framework. ~~Contrary to Gunter et al. (2013), we do not observe significant uplift in the Amundsen Sea Sector. Although a present-day viscoelastic component in the uplift, resulting from strong ice losses over the past decade, may be possible (Karato (2008)), our preliminary studies show that this uplift would probably not be as pronounced and especially not as widespread as that in Gunter et al. (2013). Rather, we assume that their result stems from an overestimation of SMB rates in the area.~~

For this proof-of-concept study, our focus lies mainly on ice dynamics, SMB and GIA estimates, neglecting to a certain extent the influence of mass-invariant height changes (due to firn compaction and elastic uplift of the bedrock). At this stage, the ~~model~~ framework ~~only reserves one field for (purely)~~ solves for a single process that combines elastic rebound ~~of the earth's crust~~ and firn compaction. In ~~the~~ this time-invariant framework, the two are confounded and cannot be separated, as they are not distinguishable by different densities or length scales. A better ~~way~~ approach to solve for the elastic rebound of the crust would be to integrate a dynamic estimate that depends on the ice load changes. This approach is being implemented in the spatiotemporal version of the ~~model~~framework. ~~The f~~Firn compaction is currently linked with SMB through a simple correlation model (Zammit-Mangion et al., 2014). This approach could be further improved by adding a temperature dependence, ~~along the lines of~~following the principles of a simple firn compaction model (Helsen et al., 2008). Finally, another open question concerns the extent of present-day viscoelastic rebound in the ~~Amundsen sea sector~~ASE. ~~The scientific community will have to wait for the official release of the POLENET GPS trends to resolve this issue~~.

6 Conclusion

~~The~~ Our proof-of-concept study shows that hierarchical modelling is a ~~valuable~~ powerful tool in separating ice mass balance, SMB and GIA processes when combining satellite altimetry, GPS and gravimetry. ~~It shows~~We demonstrate that, using only ~~minimal input from~~smoothness criteria derived from forward models, it can provide an accurate ~~and plausible~~ estimate of the different processes. A time-varying version of the framework is currently being developed, ~~several improvements for which have already been devised~~which includes a number of improvements, mentioned earlier. ~~One crucial improvement is~~In particular, ~~the dynamic~~ estimation of elastic rebound in the GPS time series, and ~~the implementation of a dynamic, if simplified firn correction mode~~more robust partitioning ~~I~~ of ice dynamics and SMB will provide substantial improvements in source separation, error reduction and GIA estimation. ~~One~~ A central advantage of the framework is that new data – which need be neither regular, ~~nor~~ or gridded – can be added at any point. For example, it ~~would be quite easy~~is possible to extend the observation period ~~to include older or younger~~forward or back in time using data ~~like~~ from ERS2, or Cryosat2, or any other data set that contains information about one of the processes being solved for. This could include, for example, accumulation radar data or shallow ice cores for SMB variability or additonal GPS sites as they become available. Preliminary tests have shown that the inference can also be performed without GRACE data. ~~Another option is to include in situ SMB data that have previously been used for validation~~.

Acknowledgements

The authors would like to thank the following colleagues for helpful discussions: Volker Klemann, Ingo Sasgen, Matt King, Liz Petrie, Pete Clarke, Martin Horwath, Finn Lindgren and Valentina Barletta. This work was funded by UK NERC grant NE/I027401/1.

Also, the following colleagues provided additional data without which the project would not have been possible: J.M. Lenaerts, S. Ligtenberg, Erik Ivins, Ricardo Riva, Brian Gunter, Pippa Whitehouse, Ingo Sasgen, Rory Bingham, Grace Nield, Liz Thomas.

References

Arthern, R. J., Vaughan, D. G., Rankin, A. M., Mulvaney, R., and Thomas, E. R.: In situ measurements of Antarctic snow compaction compared with predictions of models, Journal of Geophysical Research, 115, 2010, 10.1029/2009jf001306.

Bamber, J. L., Vaughan, D. G., & Joughin, I.: Widespread complex flow in the interior of the Antarctic ice sheet. Science, 287(5456), 1248-1250, 2000.

Bamber, J. L., Gomez-Dans, J. L., & Griggs, J. A.: A new 1 km digital elevation model of the Antarctic derived from combined satellite radar and laser data–Part 1: Data and methods. The Cryosphere, 3(1), 101-111, 2009.

Barletta, V. R., Sørensen, L. S., & Forsberg, R.:Variability of mass changes at basin scale for Greenland and Antarctica. The Cryosphere Discussions, 6(4), 3397-3446, 2012.

603 Berthier, E., Scambos, T. A., & Shuman, C. A.: Mass loss of Larsen B tributary glaciers
604 (Antarctic Peninsula) unabated since 2002. Geophysical Research Letters, 39, L13501,
605 doi:10.1029/2012GL051755 , 2012.

606 Borsa, A. A., Moholdt, G., Fricker, H. A., and Brunt, K. M.: A range correction for ICESat and its
607 potential impact on ice-sheet mass balance studies, The Cryosphere, 8, 345-357, 2014.
608
609 Burgener, L., et al.: An observed negative trend in West Antarctic accumulation rates from 1975
610 to 2010: evidence from new observed and simulated records. Journal of Geophysical Research:
611 Atmospheres, 118, 1–12, doi:10.1002/jgrd.50362, 2013.

612 Chen, J. L., et al.: "Antarctic mass rates from GRACE." Geophysical Research Letters, 33,
613 L11502, 2006.

614 Davis, C. H.: Temporal change in the extinction coefficient of snow on the Greenland ice sheet
615 from an analysis of seasat and geosat altimeter data, IEEE Trans. Geosci. Remote Sensing, 34,
616 1066-1073, 1996.

617 De Angelis, H. and Skvarca, P.: Glacier surge after ice shelf collapse, Science, 299, 1560-1562,
618 2003.
619

620 Dee, D. P., et al.: The ERA-Interim reanalysis: Configuration and performance of the data
621 assimilation system. Quarterly Journal of the Royal Meteorological Society 137.656: 553-597,
622 2011.

623 Danesi, S., and Morelli, A.: Structure of the upper mantle under the Antarctic Plate from surface
624 wave tomography. Geophysical Research Letters 28.23: 4395-4398, 2001.

625 Dobslaw, H., and Thomas, M.: Simulation and observation of global ocean mass anomalies.
626 Journal of Geophysical Research: Oceans (1978–2012), 112(C5), 2007.

627 Dobslaw, H., Flechtner, F., Bergmann-Wolf, I., Dahle, C., Dill, R., Esselborn, S., and Thomas,
628 M.: Simulating high-frequency atmosphere-ocean mass variability for dealiasing of satellite
629 gravity observations: AOD1B RL05. Journal of Geophysical Research: Oceans, 118(7), 3704-
630 3711, 2013.

631 Flament, T., & Rémy, F.: Dynamic thinning of Antarctic glaciers from along-track repeat radar
632 altimetry. Journal of Glaciology, 58(211), 830-840, 2012.

633 Fretwell, P. et al.: Bedmap2: improved ice bed, surface and thickness datasets for Antarctica. The
634 Cryosphere, 7(1), 375–393, 2013.

635 Frezzotti, M., Scarchilli, C., Becagli, S., Proposito, M., & Urbini, S.: A synthesis of the Antarctic
636 surface mass balance during the last 800 yr. The Cryosphere, 7(1), 303-319, 2013.

637 Groh, A., Ewert, H., Scheinert, M., Fritsche, M., Rülke, A., Richter, A., and Dietrich, R.: An
638 investigation of glacial isostatic adjustment over the Amundsen Sea Sector, West Antarctica.
639 Global and Planetary Change, 98, 45-53. 2012.

640 Gunter, B. C., et al.: Empirical estimation of present-day Antarctic glacial isostatic adjustment and
641 ice mass change. The Cryosphere Discuss., 7, 3497-3541, 2013.

642 Helsen, M. M., van den Broeke, M. R., van de Wal, R. S., van de Berg, W. J., van Meijgaard, E.,
643 Davis, C. H., Goodwin, I.: Elevation changes in Antarctica mainly determined by accumulation
644 variability. Science, 320(5883), 1626-1629, 2008.

645 Hofton, M. A., Luthcke, S. B., & Blair, J. B.: Estimation of ICESat intercampaign elevation biases
646 from comparison of lidar data in East Antarctica. Geophysical Research Letters, 40(21), 5698-
647 5703, 2013.

648 Horwath, M. and Dietrich, R.: Signal and error in mass change inferences from GRACE: the case
649 of Antarctica, Geophysical Journal International, 177, 849-864, 2009.

650 Hurkmans, R. T. W. L., Bamber, J. L., Davis, C. H., Joughin, I. R., Khvorostovsky, K. S., Smith,
651 B. S., and Schoen, N.: Time-evolving mass loss of the Greenland Ice Sheet from satellite
652 altimetry, The Cryosphere, 8, 1725-1740, 2014.

653 Ivins, E. R., & James, T. S.: Antarctic glacial isostatic adjustment: a new assessment. Antarctic
654 Science, 17(04), 541-553, 2005.

655 Ivins, E. R., James, T. S., Wahr, J., Schrama, O., Ernst, J., Landerer, F. W., & Simon, K. M.:
656 Antarctic contribution to sea level rise observed by GRACE with improved GIA correction.
657 Journal of Geophysical Research: Solid Earth, 118(6), 3126-3141, 2013.

658 Karato, S.: Deformation of earth materials: an introduction to the rheology of solid earth.
659 Cambridge University Press, 2008.

660 King, M. A., Bingham, R. J., Moore, P., Whitehouse, P. L., Bentley, M. J., & Milne, G. A.: Lower
661 satellite-gravimetry estimates of Antarctic sea-level contribution. Nature, 491(7425), 586-589,
662 2012.

663 Kunz, M., King, M. A., Mills, J. P., Miller, P. E., Fox, A. J., Vaughan, D. G., & Marsh, S. H.:
664 Multi-decadal glacier surface lowering in the Antarctic Peninsula. Geophysical Research Letters,
665 39(19), L19502, doi:10.1029/2012GL052823, 2012.

666 Kusche, J., Schmidt, R., Petrovic, S., & Rietbroek, R.: Decorrelated GRACE time-variable gravity
667 solutions by GFZ, and their validation using a hydrological model. Journal of Geodesy, 83(10),
668 903-913, 2009.

669 Lenaerts, J. T. M., den Broeke, M. R., Berg, W. J., Meijgaard, E. V., & Kuipers Munneke, P.: A
670 new, high-resolution surface mass balance map of Antarctica (1979–2010) based on regional
671 atmospheric climate modeling. Geophysical Research Letters, 39(4), L04501, 2012.

672 Ligtenberg, S. R. M., Helsen, M. M., and van den Broeke, M. R.: An improved semi-empirical
673 model for the densification of Antarctic firn, Cryosphere, 5, 809-819, 2011.

674 Lindgren, F., Rue, H., & Lindström, J.: An explicit link between Gaussian fields and Gaussian
675 Markov random fields: the stochastic partial differential equation approach. Journal of the Royal
676 Statistical Society: Series B (Statistical Methodology), 73(4), 423-498, 2011.

677 Luthcke, S. B., Arendt, A. A., Rowlands, D. D., McCarthy, J. J., and Larsen, C. F.: Recent glacier
678 mass changes in the Gulf of Alaska region from GRACE mascon solutions, J. Glaciol., 54, 767-
679 777, 2008.
680

681 Luthcke, S. B., et al.: Antarctica, Greenland and Gulf of Alaska land-ice evolution from an
682 iterated GRACE global mascon solution. Journal of Glaciology, 59.216, 613-631, 2013.

683 Medley, B., et al.: Airborne-radar and ice-core observations of annual snow accumulation over
684 Thwaites Glacier, West Antarctica confirm the spatiotemporal variability of global and regional
685 atmospheric models. Geophysical Research Letters 40.14: 3649-3654, 2013.

686 Moholdt, G., Nuth, C., Hagen, J. O., & Kohler, J.: Recent elevation changes of Svalbard glaciers
687 derived from ICESat laser altimetry. Remote Sensing of Environment, 114(11), 2756-2767, 2010.

688 Osmanoglu, B., Braun, M., Hock, R., & Navarro, F. J.: Surface velocity and ice discharge of the
689 ice cap on King George Island, Antarctica. Annals of Glaciology, 54(63), 111-119, 2013.

690 Peltier, W. R.: Global glacial isostasy and the surface of the ice-age Earth: The ICE-5G (VM2)
691 model and GRACE. Annu. Rev. Earth Planet. Sci., 32, 111-149., 2004.

692 Retzlaff, R., & Bentley, C. R.: Timing of stagnation of Ice Stream C, West Antarctica, from short-
693 pulse radar studies of buried surface crevasses. Journal of Glaciology, 39(133), 1993.

694 Rignot, E., Velicogna, I., Van den Broeke, M. R., Monaghan, A., & Lenaerts, J. T. M.:
695 Acceleration of the contribution of the Greenland and Antarctic ice sheets to sea level rise.
696 Geophysical Research Letters, 38(5), L05503, 2011.

697 Sasgen, I., Martinec, Z., & Bamber, J.: Combined GRACE and InSAR estimate of West Antarctic
698 ice mass loss. Journal of Geophysical Research: Earth Surface (2003–2012), 115(F4), 2010.

699 Sasgen, I., et al.: Antarctic ice-mass balance 2003 to 2012: regional reanalysis of GRACE satellite
700 gravimetry measurements with improved estimate of glacial-isostatic adjustment based on GPS
701 uplift rates. The Cryosphere Discuss., 6, 3703-3732, 2012.

702 Scambos, T. A., Bohlander, J. A., Shuman, C. U., & Skvarca, P.: Glacier acceleration and
703 thinning after ice shelf collapse in the Larsen B embayment, Antarctica. Geophysical Research
704 Letters, 31(18), L18402, 2004.

705 Shepherd, A. et al.: A reconciled estimate of ice-sheet mass balance. Science, 338(6111), 1183-
706 1189, 2012.

707 Sørensen, Louise Sandberg, et al.: Mass balance of the Greenland ice sheet (2003–2008) from
708 ICESat data - the impact of interpolation, sampling and firn density. The Cryosphere, 5, 173-186,
709 2011.

Swenson, S., Chambers, D., & Wahr, J.: Estimating geocenter variations from a combination of GRACE and ocean model output. Journal of Geophysical Research: Solid Earth (1978–2012), 113(B8), 2008.

Tapley, B. D., Bettadpur, S., Ries, J. C., Thompson, P. F., & Watkins, M. M.: GRACE measurements of mass variability in the Earth system. Science, 305(5683), 503-505, 2004.

Van de Berg, W. J., van den Broeke, M. R., van Meijgaard, E., and Reijmer, C. H.: Reassessment of the Antarctic surface mass balance using calibrated output of a regional atmospheric climate model, J Geophys Res, 111, D11104, doi:10.1029/2005JD006495, 2006.

Velicogna, I., & Wahr, J.: Measurements of time-variable gravity show mass loss in Antarctica. science, 311(5768), 1754-1756, 2006.

Werth, S., Güntner, A., Schmidt, R., & Kusche, J.: Evaluation of GRACE filter tools from a hydrological perspective. Geophysical Journal International, 179(3), 1499-1515, 2009.

Whitehouse, P. L., Bentley, M. J., Milne, G. A., King, M. A., & Thomas, I. D.: A new glacial isostatic adjustment model for Antarctica: calibrated and tested using observations of relative sea-level change and present-day uplift rates, 2012.

Wouters, B., Chambers, D., & Schrama, E. J. O.: GRACE observes small-scale mass loss in Greenland. Geophysical Research Letters, 35(20), L20501, 2008.

Yan, X. Linear regression analysis: theory and computing. World Scientific, 2009.

Zammit-Mangion, A., Rougier, J., Bamber, J., and Schön, N.: Resolving the Antarctic contribution to sea-level rise: a hierarchical modelling framework, Environmetrics, 25, 245-264, 2014.~~Zammit Mangion, A. et al.: Resolving the Antarctic contribution to sea level rise: a hierarchical modelling framework, Environmetrics, 2013~~.

Zammit-Mangion, A., Bamber, J. L., Schoen, N. W., and Rougier, J. C.: A data-driven approach for asessing ice-sheet mass balance in space and time, Annals of Glaciology, 56, XXX, 2015.

Zwally, H. J., and Brenner, A. C.: Ice sheet dynamics and mass balance. International Geophysics, 69, 351-xxvi, 2001.

Zwally, H. et el.: GLAS/ICESat L2 Antarctic and Greenland Ice Sheet Altimetry Data. Version 33. Boulder, Colorado USA: National Snow and Ice Data Center, 2011.

Formatted: Font: (Default) Times New Roman, 12 pt

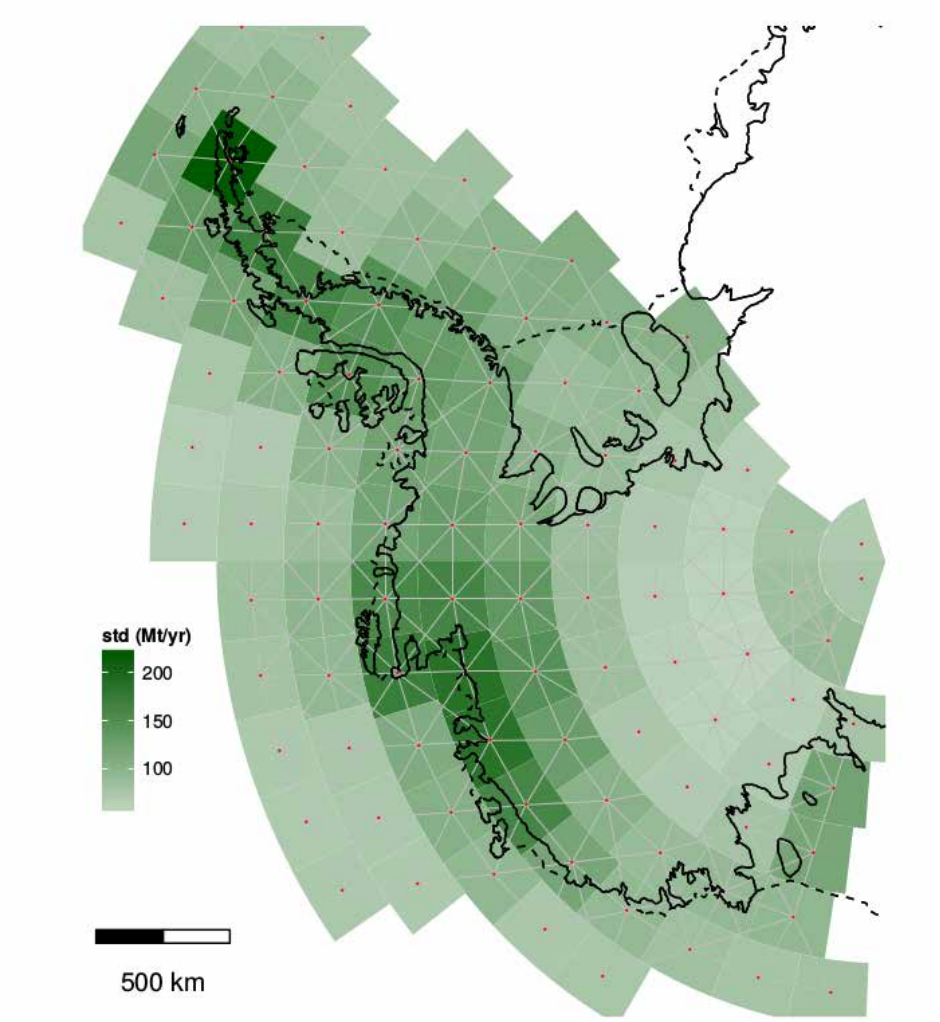

Figure 1. Error estimates for the GRACE mascon solutions, derived from a regression of the data (Zammit-Mangion, et al, 2014).

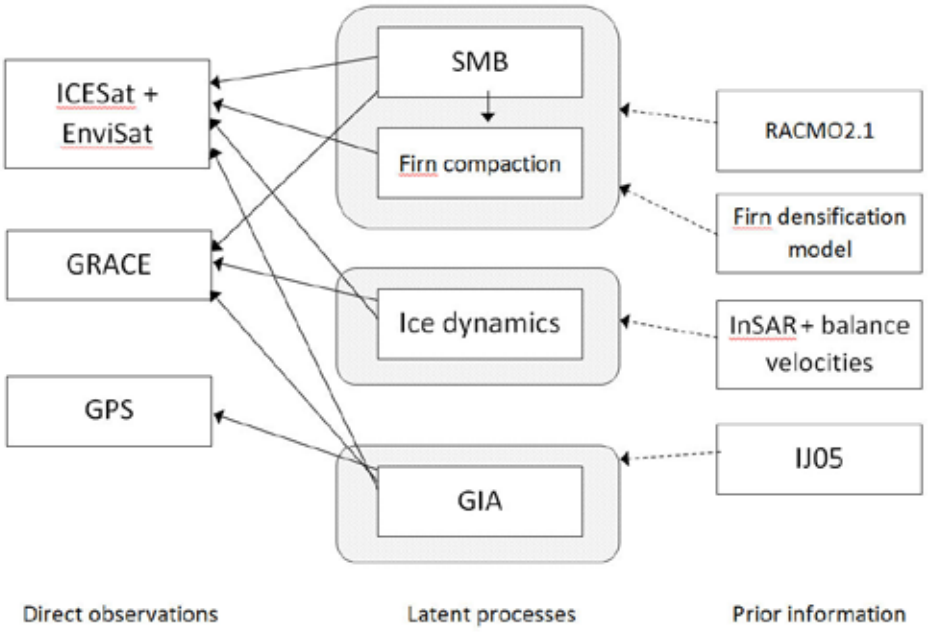

Figure 2. Schematic diagram showing the relationship between the observations, process model defining the latent processes and the priors employed.

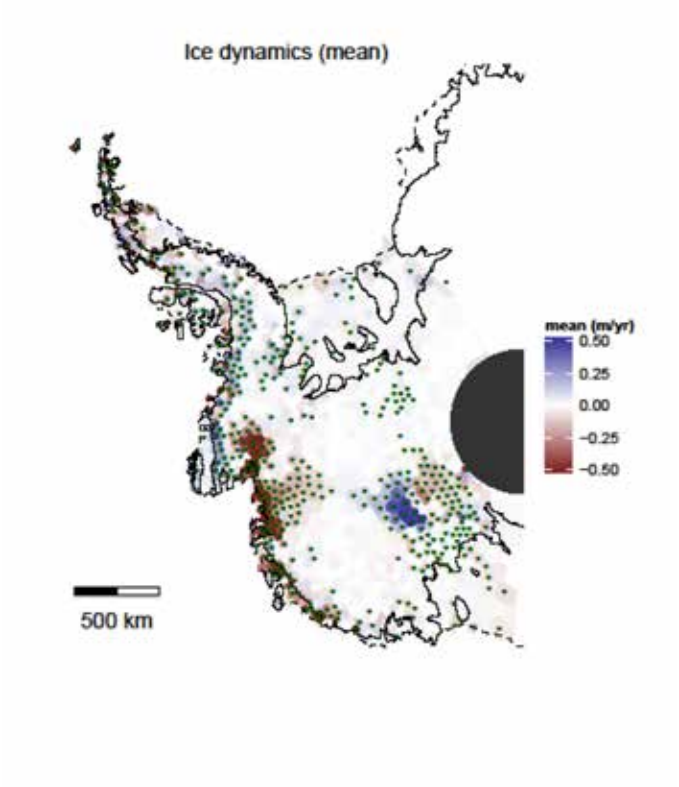

753

754

755 Figure ~~3~~1a. Ice dynamics for 2003–2009 in m/yr. Stippled points denote areas in which the mean
756 signal is larger than the marginal standard deviation.

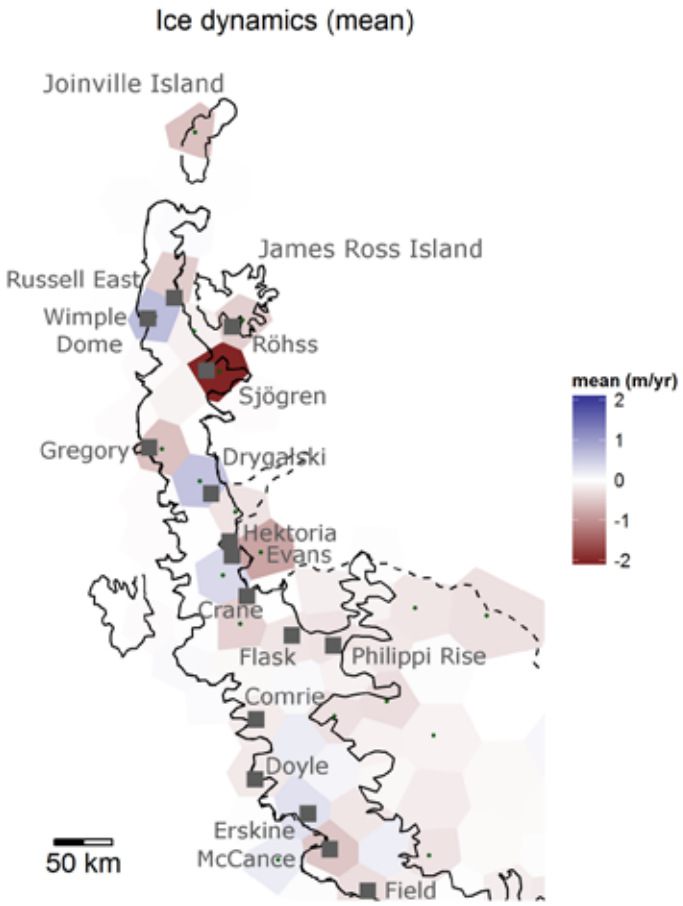

757

758 Figure ~~3~~1b. Ice dynamics for 2003–2009 in m/yr. Close-up for the Northern Antarctic Peninsula,
759 with glacier locations (grey squares). ~~Stippled points denote areas in which the mean signal is~~
760 ~~larger than the marginal standard deviation.~~

761

762

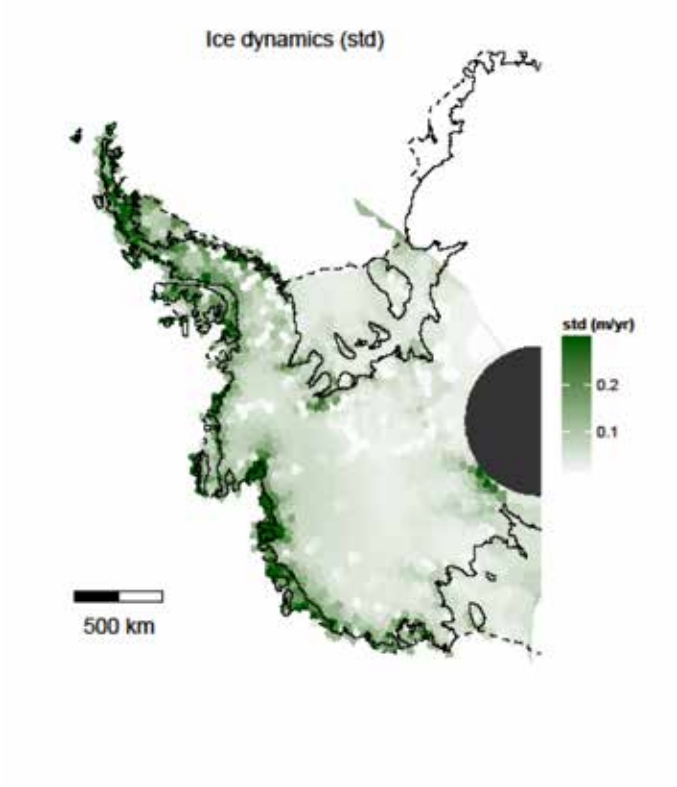

Figure 4~~2~~. Marginal standard deviation of ice dynamics for 2003–2009 in m/yr.

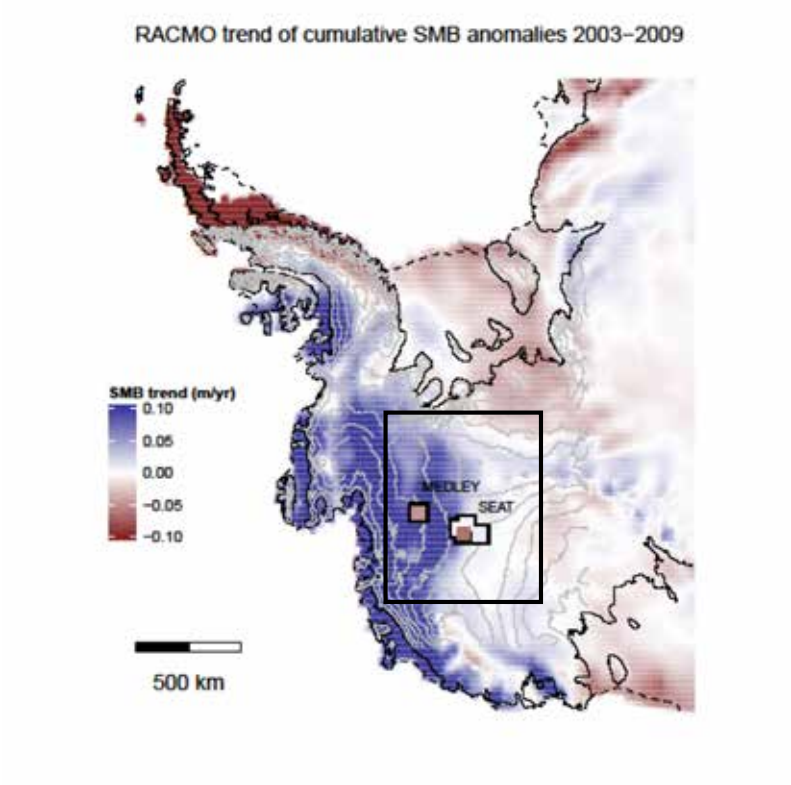

765

766

767 Figure ~~5~~3. The SMB trend for 2003–2009 as obtained from RACMO. Contour lines (shown from
768 -1000 to 1000km Northing) are elevations from BEDMAP surface (Fretwell et al., 2013). Mean
769 ice core accumulation rates from Medley et al. (2013) (denoted MEDLEY) and ice core
770 accumulation rates from Burgener et al. (2013) (denoted SEAT). Rectangle shows area in close-up
771 (Fig. 5).

772

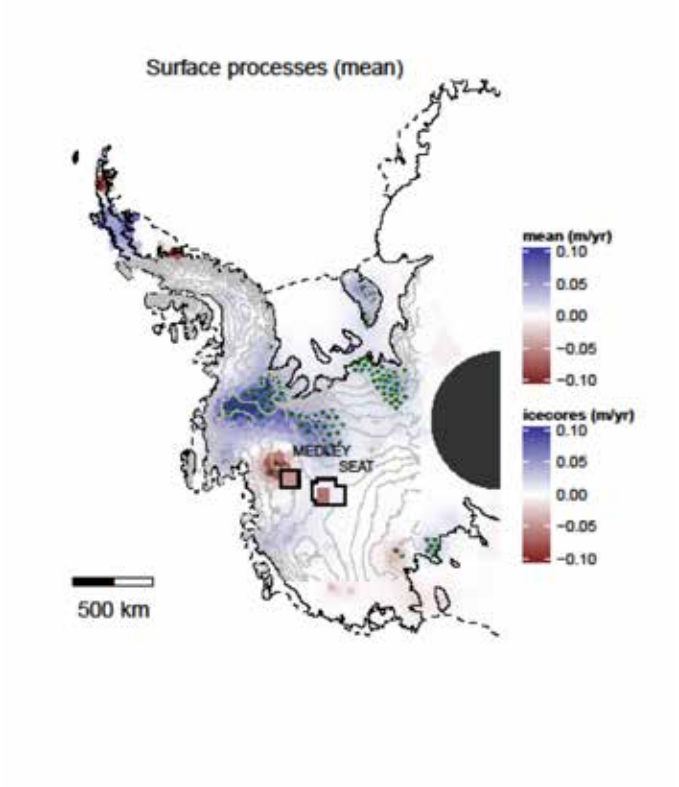

Figure 64. SMB rates for 2003–2009 in m/yr and locations of the ice cores from Burgener et al. (2013) and Medley et al. (2013). Contour lines ~~(shown from −1000 to 1000km Northing)~~ are elevations from the BEDMAP surface (Fretwell et al., 2013). Stippled points denote areas in which the mean signal is larger than the marginal standard deviation.

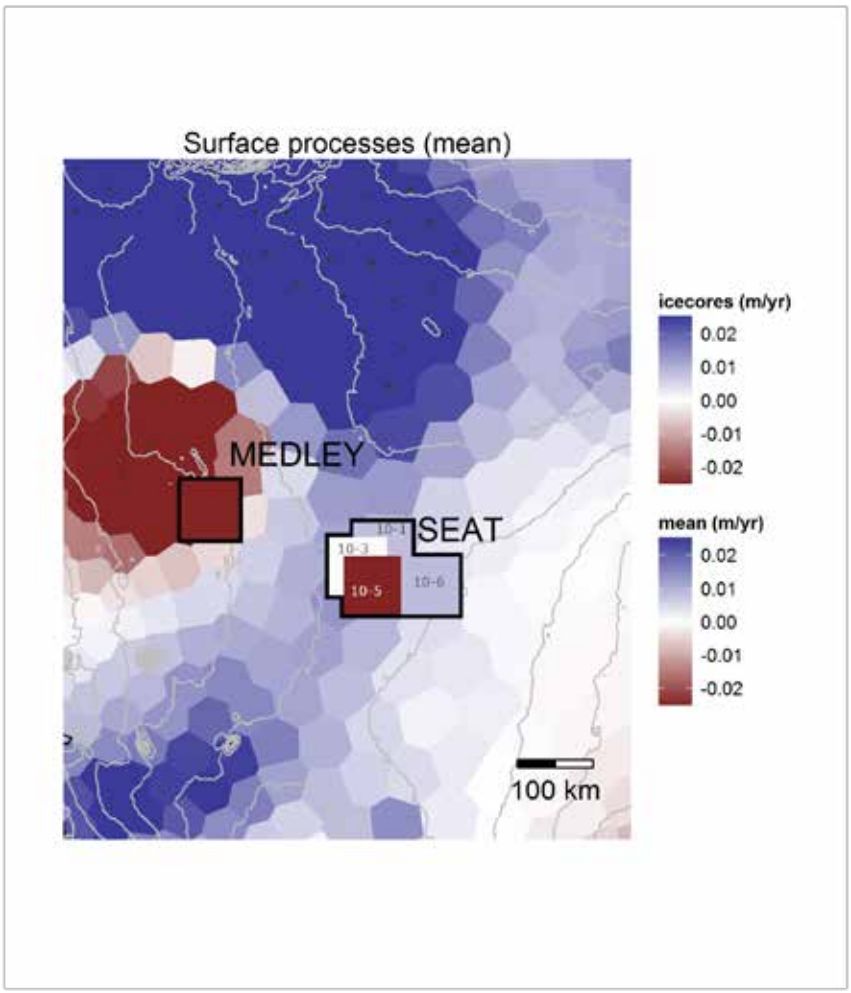

780

781 Figure 7~~5~~. Close-up of ice core mean from Medley et al. (2013) (denoted MEDLEY) and ice
782 cores from Burgener et al. and RATES SMB trends for 2003–2009 in the Amundsen Sea
783 Embayment. Numbers denote SEAT ice cores 10-1, 10-3, 10-5, and 10-6. Contour lines are
784 elevations from BEDMAP surface (Fretwell et al., 2013). Stippled points denote areas in which
785 the mean signal is larger than the marginal standard deviation.

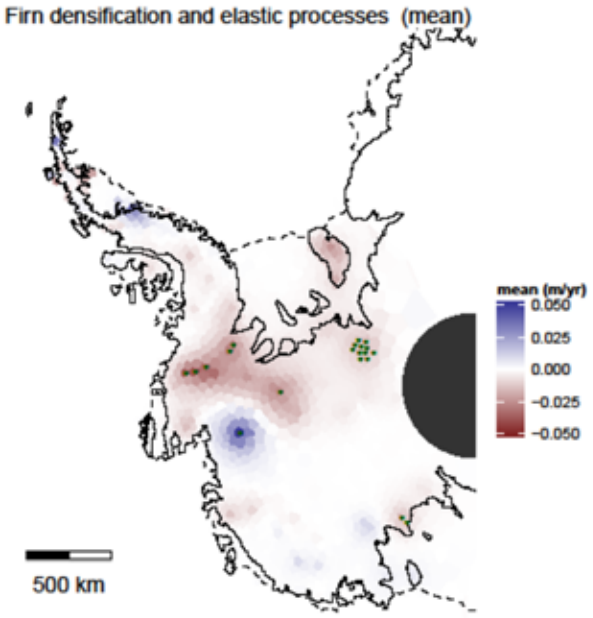

786

787 Figure ~~8~~6. Height changes from firn compaction and elastic uplift of the crust for 2003–2009 in
788 m/yr. Stippled points denote areas in which the mean signal is larger than the marginal standard
789 deviation.

790

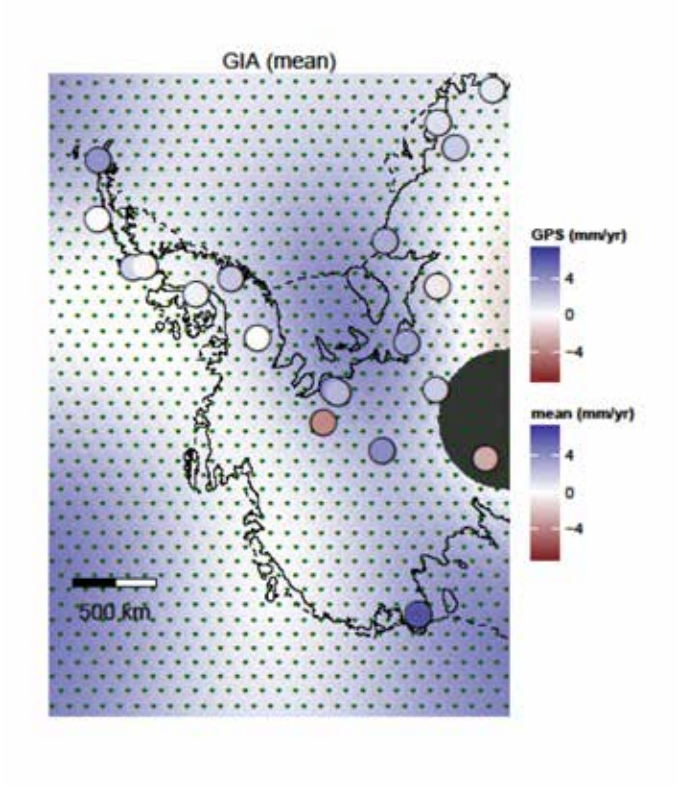

Figure 9~~7~~. GIA estimate with GPS stations and their rates. Stippled points denote areas in which the mean signal is larger than the marginal standard deviation.

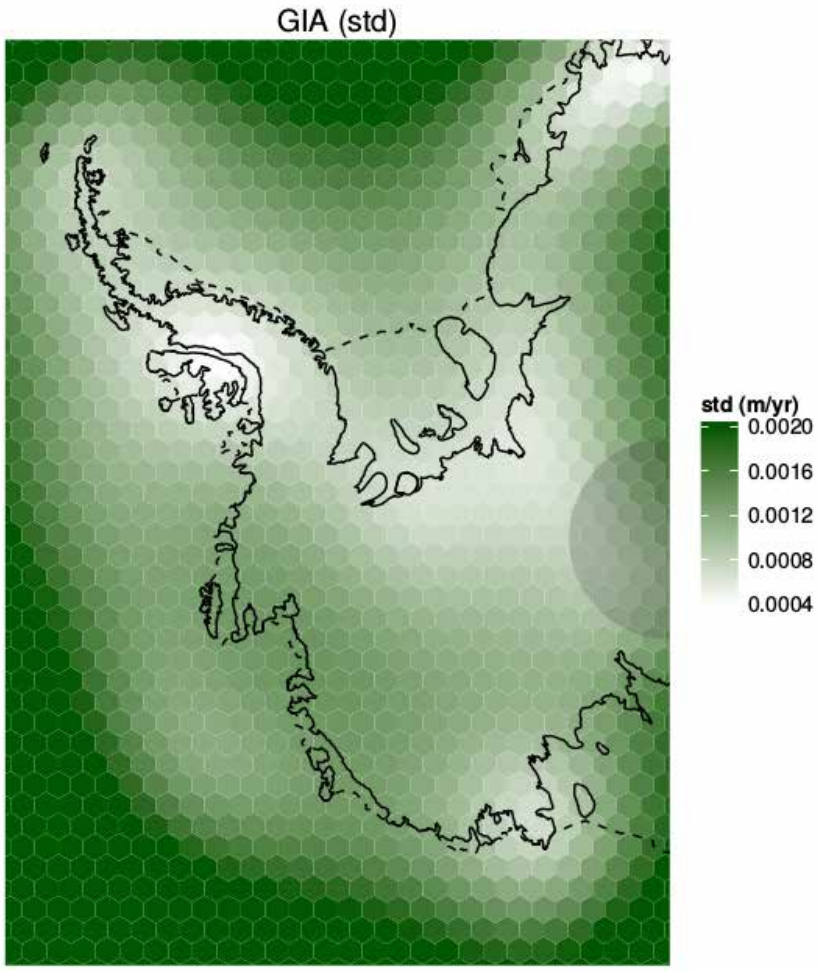

Figure 10. GIA error estimate (one standard deviation).

Formatted: Font: Not Italic

Formatted: Font: Not Italic

Formatted: Font: Not Italic

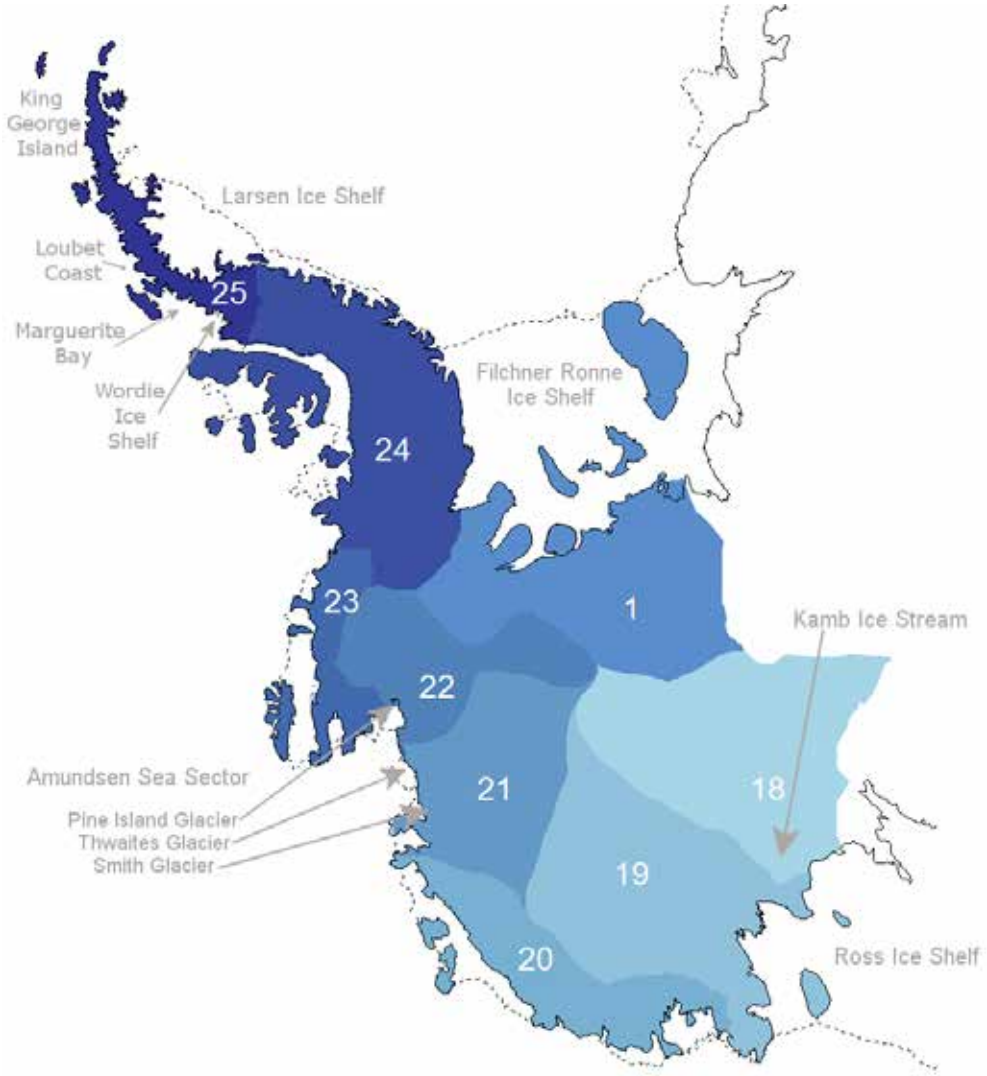

798

799 Figure 11~~8~~. Basin definitions used for West Antarctica (adapted from Sasgen et al., 2013).

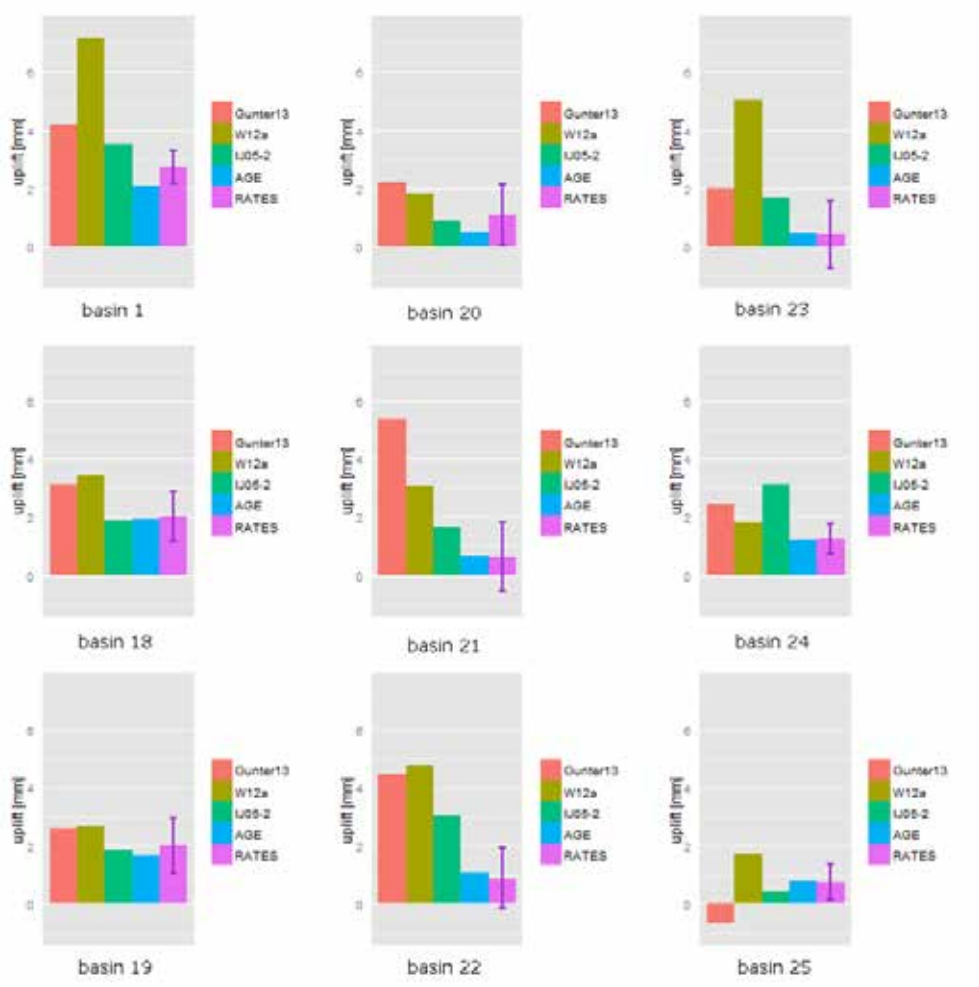

Figure 12~~9~~. Comparison of RATES results with different GIA estimates and forward models.

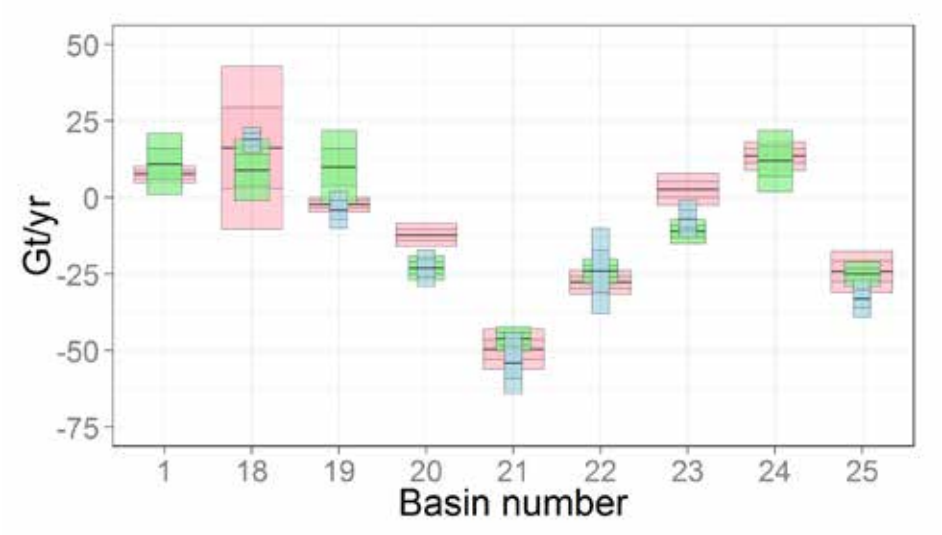

Figure 1~~3~~0. Combined Ice and SMB loss trends for West Antarctica using RATES (pink), results from King et al. (2013)(blue), and from Sasgen et al. (2013) (green). Basin definitions for King et al. (2012) differ for basins 1 and 24, so they are given in Table 3~~2~~ instead. Our basin 25 is equal to the sum of basins 25 and 26 in King et al. (2012), this is given here as basin 25 for the King estimate.

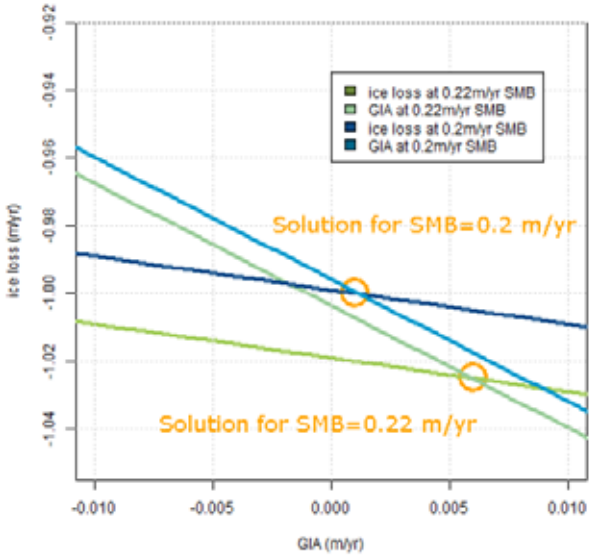

Figure 1~~4~~1. Toy example illustrating the sensitivity of combination methods to differing SMB estimates. The blue lines represent the set of equations that solve for ice loss and GIA when SMB=0.2 m/yr. The green lines represent the equations for SMB=0.22 m/yr.

Table 1. GPS stations with vertical rate and errors, modelled elastic correction and adjusted rates. The latter are used for inference.

Site Name	Lat	Lon	Start Year	Start Day of year	End Year	End Day of year	data days	GPS rate (mm/yr)	Sigma	modelled elastic	adjusted GPS
ABOA	-73.04	346.59	2003	31	2010	11	1959	1.4	0.84	0.27	1.13
BELG	-77.86	325.38	1998	33	2005	45	1517	2.97	1.47	0.02	2.95
BREN	-72.67	296.97	2006	362	2010	194	463	3.85	1.6	1.85	2
FOS1	-71.31	291.68	1995	35	2010	364	317	2.14	0.4	1.64	0.5
MBL1_AV	-78.03	204.98						3.28	1.09	0.28	3
OHIG	-63.32	302.1	1995	69	2002	48	1667	3.8	1	NULL	3.8
PALM	-64.78	295.95	1998	188	2002	59	1181	0.08	1.87	NULL	0.08
ROTB	-67.57	291.87	1999	54	2002	59	239	1.5	1.9	NULL	1.5
SMRT	-68.12	292.9	1999	112	2002	59	751	-0.22	1.93	NULL	-0.22
SVEA	-74.58	348.78	2004	317	2008	20	1030	2.07	1.95	0.24	1.83
VESL	-71.67	357.16	1998	212	2010	328	3081	1.06	0.45	0.25	0.81
W01_AV	-87.42	210.57						-2.8	1.17	-0.09	-2.71
W02_AV	-85.61	291.45						2.17	1	0.28	1.89
W03_AV	-81.58	331.6						-2.47	1.28	-1.73	-0.74
W04_AV	-82.86	306.8						3.42	0.84	0.16	3.26
W04B/CRDI	-82.86	306.8	2002	358	2008	24	16	4.06	1.32	0.16	3.9
W06A	-79.63	268.72	2002	356	2005	358	12	-2.2	2.42	1.53	-3.73
W07_AV	-80.32	278.57						3.61	1.58	0.97	2.64
W09	-82.68	255.61	2003	9	2006	8	34	4.54	2.59	0.49	4.05
W12A/PATN	-78.03	204.98	2003	331	2007	363	17	6.41	1.61	0.28	6.13
W08A/B/SUGG	-75.28	287.82	2003	3	2006	4	13	1.31	1.28	1.3	0.01

Table 2. Prior information and soft constraints applied to length-scales and amplitudes based on expert judgement and analysis of the forward models discussed in section 2.4

Formatted: Font: Not Italic

Process	**Length scale**	**Softly constrained amplitude (1sigma)**	**Dependency**
GIA	3000 km	5mm/yr	Independent
Ice dynamics	50 km	1 mm/yr in interior – 15m/yr in areas flowing faster than ~15 m/yr	Independent
Firn compaction	80 km at coast – 200 km at interior	1 mm/yr in interior – 140 mm/yr at coast	Anti-correlated with SMB (rho = -0.4)
SMB	80 km at coast – 200 km at interior	1 mm/yr in interior – 240 mm/yr at coast	Anti-correlated with firn compaction (rho = -0.4)

Table 4. Mass trend values for each basin shown in Figure 8 for different values of the GIA length scale, SMB length scale and ice surface velocity threshold. All values in colums 2-4 are in Gt/yr.

Formatted: Font: Not Italic

Basin Number	Original mass trend	GIA length scale 1000 km	SMB length scale from RACMO: 150 km everywhere	Ice horizontal velocity threshold 50 m/yr
01	7.57 ± 1.41	7.49 ± 1.40	8.11 ± 1.36	5.40 ± 1.0
18	16.16 ± 13.26	13.48 ± 12.92	15.12 ± 13.05	24.80 ± 3.18
19	-2.24 ± 1.19	-2.23 ± 1.26	-2.18 ± 1.29	-0.71 ± 0.91
20	-12.22 ± 1.94	-11.47 ± 1.98	-12.28 ± 1.93	-13.21 ± 1.67
21	-49.48 ± 3.32	-45.31 ± 3.56	-49.53 ± 3.41	-47.01 ± 3.38
22	-27.62 ± 1.95	-26.34 ± 2.02	-27.34 ± 1.90	-24.12 ± 1.75
23	2.68 ± 2.65	3.28 ± 2.67	2.62 ± 2.65	-0.18 ± 2.59
24	13.57 ± 2.28	13.65 ± 2.30	13.39 ± 2.30	7.92 ± 1.67
25	-24.09 ± 3.39	-24.75 ± 3.20	-24.43 ± 3.42	-8.09 ± 1.90

Table 3~~2~~. Ice and SMB mass trends from RATES, Sasgen et al. (2013), and King et al. (2012), in GT/yr. *Our basin 25 is equal to the sum of basins 25 and 26 in King et al. (2012). The sum of our basins 1 and 24 is equal to their sum of basins 1, 24, and 27.

Basin	RATES 03/2009-10/2009	Sasgen (2013) 03/2009-10/2009	King (2012) 2002–2010	Diff RATES-Sasgen	Diff RATES-King
1	7.6	11	-	**-3.4**	-
18	16.2	9.5	19.2	**6.7**	**-3**
19	-2.2	10	-4	**-12.2**	**1.8**
20	-12.2	-23	-23	**10.8**	**10.8**
21	-49.5	-46	-54	**-3.5**	**4.5**
22	-27.6	-24	-24	**-3.6**	**-3.6**
23	2.7	-11	-7	**13.7**	**9.7**
24	13.6	12	-	**1.6**	**-**
25 (25+26)*	-24.1	-25	-33	**0.9**	**8.9**
(1+24+27)*	21.2	23	8.5	**-1.8**	**12.7**
WAIS	**-75.5**	**-86.5**	**-117.3**	**9.2**	**41.8**